



Genome-wide association study reveals new genes involved in leaf trichome formation in polyploid oilseed rape (*Brassica napus* L.)

Lijie Xuan¹ | Tao Yan¹ | Lingzhi Lu¹ | Xinze Zhao¹ | Dezhi Wu¹ | Shuijin Hua² | Lixi Jiang¹

¹ Provincial Key Laboratory of Crop Gene Resources, Zhejiang University, Hangzhou, China

² Institute of Crop and Nuclear Technology Utilization, Zhejiang Academy of Agricultural Sciences, Hangzhou, China

Correspondence

Lixi Jiang, Provincial Key Laboratory of Crop Gene Resources, Zhejiang University, Hangzhou 310058, China.

Email: jianglx@zju.edu.cn

Funding information

Natural Science Foundation of China, Grant/Award Number: 31671597; Jiangsu Collaborative Innovation Centre for Modern Crop Production, Grant/Award Number: B17039; Fundamental Research Funds for the Central Universities, Grant/Award Number: 2019FZA6011; National Key Basic Research Project, Grant/Award Number: 2015CB150205

Abstract

Leaf trichomes protect against various biotic and abiotic stresses in plants. However, there is little knowledge about this trait in oilseed rape (*Brassica napus*). Here, we demonstrated that hairy leaves were less attractive to *Plutella xylostella* larvae than glabrous leaves. We established a core germplasm collection with 290 accessions for a genome-wide association study (GWAS) of the leaf trichome trait in oilseed rape. We compared the transcriptomes of the shoot apical meristem (SAM) between hairy- and glabrous-leaf genotypes to narrow down the candidate genes identified by GWAS. The single nucleotide polymorphisms and the different transcript levels of *BnaA.GL1.a*, *BnaC.SWEET4.a*, *BnaC.WAT1.a* and *BnaC.WAT1.b* corresponded to the divergence of the hairy- and glabrous-leaf phenotypes, indicating the role of sugar and/or auxin signalling in leaf trichome initiation. The hairy-leaf SAMs had lower glucose and sucrose contents but higher expression of putative auxin responsive factors than the glabrous-leaf SAMs. Spraying of exogenous auxin (8 µm) increased leaf trichome number in certain genotypes, whereas spraying of sucrose (1%) plus glucose (6%) slightly repressed leaf trichome initiation. These data contribute to the existing knowledge about the genetic control of leaf trichomes and would assist breeding towards the desired leaf surface type in oilseed rape.

KEY WORDS

auxin signalling, RNA-seq analysis, sugar signalling

1 | INTRODUCTION

Plant trichomes that cover various tissues, such as leaves, stems and fruits, evolve from epidermal cells. Surface trichomes have several advantages. First, trichomes shield plants from herbivore damage by forming a hairy. Second, trichomes, mainly leaf trichomes, reduce transpiration in dry conditions by breaking up the flow of air across the leaf surface. Third, a coating of dense trichomes on the leaf surface protects the delicate tissues underneath from ultraviolet-light exposure (Benz & Martin, 2006; Ehleringer, Bjorkman, & Mooney, 1976; Hauser, 2014;

Koudounas, Manioudaki, Kourti, Banilas, & Hatzopoulos, 2015; Plett, Wilkins, Campbell, Ralph, & Regan, 2010; Stefanowicz et al., 2016). However, in cases in which plant leaves are consumed as fodder or vegetables, trichomes can be a source of phytochemicals producing specific flavours but also may cause an unpleasant mouthfeel.

To date, most of the knowledge about the genetic control of trichome development has been gained from *Arabidopsis* (*Arabidopsis thaliana*) plants, which have dense trichomes on the leaf and stem surfaces. In *Arabidopsis*, more than 30 genes are involved in the control of trichome initiation and development. Of these, three protein families, namely, the WD40 repeat proteins (e.g., TRANSPARENT TESTA GLABRA1 (TTG1) (Walker et al., 1999)), the R2R3 MYB-related

Lijie Xuan and Tao Yan contributed equally to this study.

transcription factors (TFs) (such as GLABRA1 [GL1], MYB5 and MYB23 (Kirik, 2005; Oppenheimer, Herman, Sivakumaran, Esch, & Marks, 1991; Tominaga-Wada et al., 2012)) and the bHLH proteins (including GLABRA3 (GL3), ENHANCER OF GLABRA3 (EGL3) and TRANSPARENT TESTA 8 (TT8) (Payne, Zhang, & Lloyd, 2000; Zhang, 2003)) are known to play important roles in trichome development. Typically, these proteins make up a trimeric activator complex, namely, the MYB bHLH-WD40 (MBW) complex, which positively regulates downstream genes and induces trichome initiation. Phytohormones, that is, gibberellins (GA), jasmonic acid (JA) and brassinosteroids (BR), are involved in trichome initiation and development. Evidence shows that upon perception of a GA signal, protein–protein interactions between DELLA-GL1/GL3/EGL3 are disrupted, as DELLA proteins, in particular RGA and RGL2, are degraded by the 26S proteasome system, leading to the release of GL1/GL3/EGL3 and the formation of a complex with TTG1, which activates GL2 expression and consequently mediates trichome initiation (Qi et al., 2014). In addition, the protein–protein interaction between the JA-ZIM domain protein and GL3/EGL3/GL1 is disrupted upon perception of JA signalling, after which GL1/GL3/EGL3 are released to form the MBW complex with TTG1 (Chini et al., 2007; Qi et al., 2014). Trichome development is also influenced by BRs. *bis1* plants, which were defective in BR response, grew fewer trichomes on their leaves, suggesting a role for BRs in trichome development (Laxmi, Paul, Peters, & Khurana, 2004). There are a few studies reporting the role of auxin in trichome development. Increased auxin levels or high expression of auxin responsive factors (ARFs) leads to dense trichomes in tomato and orchidaceae (Novak & Whitehouse, 2013; Zhang et al., 2015).

A close relative of *Arabidopsis* in the family Brassicaceae, oilseed rape (*Brassica napus* L.), is an important source of edible oil in many parts of the world. Healthy seedling growth could be secured by seed dressing, a technology that treats seeds with pesticides and/or fungicides prior to planting (Jameson, 1960; Khanzada, Rajput, Shah, Lodhi, & Mehbob, 2002). However, the loss of pesticide (or fungicide) efficacy may result in damage to seedlings and tremendous yield loss, which has occurred in some European countries in recent years. Thus, an ideal strategy to protect young seedlings from insect damage may be breeding varieties with dense leaf hairs. *B. napus* is an allopolyploid (AACC, $2n = 4X = 38$) originating from an interspecific hybridization between *Brassica rapa* (AA) ($2n = 2X = 20$) and *B. oleracea* (CC) ($2n = 2X = 18$) less than 7,500 years ago (Chalhoub et al., 2014; Wu et al., 2019). Thus, in parallel to a single *Arabidopsis* gene, there normally exist 2–10 orthologous copies, which are by no means all functional. The genome rearrangement in the process of polyploidy gave rise to biased expression of functional genes between the two subgenomes and a considerable proportion of pseudogenes. In contrast to the trichomes in *Arabidopsis*, the trichomes in oilseed rape are normally unbranched and are more easily observed on seedling leaves than on adult leaves, suggesting different molecular mechanisms regulating trichome initiation and development (Alahakoon et al., 2016; Schellmann & Hulskamp, 2005). It is difficult to develop efficient technologies, such as the T-DNA or Ds/Ac insertional tagging systems in *Arabidopsis* or rice, to identify functional genes in oilseed rape because of its polyploid genome and redundant copies of functional genes. To deal with this issue, a genome-wide association study (GWAS)

is an effective strategy to identify candidate genes that control agronomic and quality traits in polyploid oilseed rape. The rapid development of sequencing technologies has facilitated the identification of single nucleotide polymorphisms (SNPs) and other genetic variations in a population (Du et al., 2018; Wang et al., 2017; Wu et al., 2019). Linkage disequilibrium (LD) is the nonrandom association of alleles at different loci in a population, and an LD map is normally drawn to indicate the degree of correlation between various loci, that is, between significant SNPs and candidate functional genes (Slatkin, 2008; Wei et al., 2017; Wu et al., 2019).

In a recent study, we resequenced a worldwide collection of 991 *B. napus* genetic materials originating from 39 countries. We identified the worldwide pattern of genetic polymorphisms in *B. napus* and unveiled the genetic basis of ecotype divergence in this crop species (Wu et al., 2019). In this study, we established a core germplasm collection including 290 accessions, representing 97.3% of the SNPs and 97.9% of the indels of the 991-accession collection, for GWAS on leaf trichome initiation in oilseed rape. To narrow down the candidate genes identified by GWAS, we compared the shoot apical meristem (SAM) transcriptomes between typical hairy- and glabrous-leaf accessions. We found that the SNP patterns and the different transcript levels of *BnaA.GL1.a*, *BnaC.SWEET4.a*, *BnaC.WAT1.a* and *BnaC.WAT1.b* corresponded to the divergence of hairy- and glabrous-leaf genotypes. In *Arabidopsis*, SWEET4 mediates sugar transport to axial sinks and affects plant development (Liu, Zhang, Yang, Tian, & Li, 2016). WALLS ARE THIN1 (WAT1), a plant-specific protein that dictates secondary cell wall thickness of wood fibres, is a vacuolar auxin transport facilitator required for auxin homoeostasis (Ranocha et al., 2013). The orthologous genes such as *BnaC.SWEET4.a*, *BnaC.WAT1.a* and *BnaC.WAT1.b* imply roles for sugar and auxin signalling in leaf trichome development in *B. napus*.

2 | METHODS

2.1 | Plant materials and growth conditions

The 290 core accessions of *B. napus* germplasm were selected from a worldwide germplasm collection of 991 accessions based on phylogenetic and principal component analyses. The 290 core accessions were grown in the experimental field of Changxing Agricultural Experiment Station of Zhejiang University ($30^{\circ}02'N$ and $119^{\circ}93'E$) (Location 1) and Zi-Jin-Gang Campus of Zhejiang University ($30^{\circ}17'N$ $120^{\circ}05'E$) (Location 2) during the oilseed rape production season from October 2017 to May 2018. The genetic materials had been sown in nursery beds in plastic tunnels before they were transplanted into the open field. Twelve plants of each accession were transplanted in a block ($160 \times 40 \text{ cm}^2$) with three replicates. Accessions with more than 50 visible hairs on the second true leaf were recorded as 'hairy-leaf (H) type', and accessions without hairs or with fewer than 50 visible hairs on the second leaf were noted as 'glabrous-leaf (G) type'. The second true leaves of the seedlings were collected for photography. A Leica stereomicroscope (Leica DFC300 FX, Wetzlar, Germany) was used for trichome observation and photography.

2.2 | Assays of *P. xylostella* larvae feeding preference

Three typical hairy-leaf accessions (Nos. 741, 988 and 1081) and three glabrous-leaf accessions (Nos. 399, 671 and 1031) of oilseed rape were selected for the diamondback moth (*P. xylostella*) feeding experiment (Table S1). *P. xylostella* larvae were provided by the Institute of Entomology of Zhejiang University. The larvae were originally captured from a local cabbage field (30.3009 N 120.0870 E, Hangzhou, China) and further reared on cabbage in a growth chamber conditioned at 25°C, 65% relative humidity, and 14 hr light/10 hr dark photoperiod. The first and second true leaves were randomly selected for the feeding experiment 2–3 weeks after sowing. Fourth-instar *P. xylostella* larvae were starved for 5–6 hr before they were transferred into Petri dishes supplied with oilseed rape leaves. The hairy and glabrous leaves were either placed in separate dishes or arranged side by side as alternatives in the same dish. The Petri dishes (12 × 12 × 2 cm³) were perforated in advance to ensure the circulation of air. The area of consumed leaves in the separate dishes was measured after 6 hr, whereas the area of consumed leaves in the combined dishes was measured after an overnight (10–12 hr) feeding. The consumed areas were measured using Photoshop software (Adobe Photoshop CC 2018 v19.1.5.61161 x32/x64). The targeted areas were captured and the pixels of the areas were automatically recorded.

2.3 | Genome-wide association study

The SNPs among the 290 accessions were extracted from the total SNPs of the 991 accessions, which was identified in our previous study (Wu et al., 2019). A total of 2,705,480 high-quality SNPs (MAF > 0.05, missing rates <0.5) were used for the GWAS. Principal component analysis (PCA) was performed using the smartPCA program from the EIGENSOFT package (<https://github.com/DReichLab/EIG; v.6.0.1>), and the top three PCs were used to construct the Q matrix for population-structure correction. The K-value, which represents the genetic relations between samples, was calculated by Plink software (Purcell et al., 2007; www.cog-genomics.org/plink2; v1.9). TASSEL software (Bradbury et al., 2007; <http://www.maizegenetics.net/tassel>) with a mixed linear model (MLM) was applied to test the associations. Both Q- and K-values were used in the MLM. The *p*-value of each SNP was calculated, and $-\log_{10}p > 6$ was defined as the suggestive threshold. Then, 100 kb sequence regions adjacent to the significantly associated SNPs were searched for associated genes.

2.4 | Analyses of genomic sequences

A total of 282 accessions were selected from the 290 accessions to analyse the distribution of SNPs in the genomic regions of the candidate genes. Eight accessions were eliminated from the SNP distribution analysis because of their inconstant phenotype of trichome appearance between the two experimental locations. The SNPs

generated by mapping the resequenced genomes to the 'Darmor-bzh' reference genome (Chalhoub et al., 2014) were compared between the hairy- and glabrous-leaf groups. The numbers '0' and '1' represent the SNPs homozygous (0) and heterozygous (1) to the reference alleles, respectively, whereas the number '2' represents the SNPs homozygous to the nonreference alleles.

The sequences of the genomic regions ~3 kb upstream of the CDSs of the MYB genes were obtained from the *Brassica napus* Genome Brower (<http://www.genoscope.cns.fr>) and analysed by using Plant CARE (<http://bioinformatics.psb.ugent.be/webtools/plantcare/html/>) (Lescot et al., 2002).

2.5 | Case-control association analysis

The Haplovew software package, in particular the permutation test program, was used to identify significantly associated individual alleles in the case-control association analysis. *p*-Values were corrected for multiple testing by means of permutation analysis. A total of 100,000 permutations were performed to correct the *p*-values. Values less than 0.001 was set as the statistically significant threshold (Barrett, Fry, Maller, & Daly, 2005).

2.6 | RNA-seq analysis

SAM tissues (before true leaves growing out) of three typical hairy accessions (Nos. 741, 988 and 1081) and three typical glabrous accessions (Nos. 399, 987 and 1031) were harvested for RNA extraction and the subsequent RNA-seq and real-time quantitative PCR (RT-qPCR) experiments. Total RNA was extracted using an RNA Extraction Kit (Cat No. R6827-1, Omega). RNA-seq was performed by Biomarker Technology Co. (Beijing, China). Sequencing libraries were generated using the NEBNext Ultra RNA Library Prep Kit for Illumina (NEB, Ipswich) according to the manufacturer's instructions. The library preparations were sequenced on an Illumina HiSeq 2500 platform, and paired-end reads were generated. The adaptor sequences and low-quality sequence reads were removed from the data sets. Clean reads were subsequently mapped to the *B. napus* reference genome using Hisat2 software (Kim, Langmead, & Salzberg, 2015). The expression levels of the genes in glabrous- and hairy-leaf SAMs were normalized to fragments per kilobase per million. Differential expression analysis of two samples was performed using the R package DESeq2 (Love, Huber, & Anders, 2014). The resulting *p* values were adjusted using Benjamini and Hochberg's approach for controlling the false discovery rate (FDR). The parameters (FDR < 0.05 and $|\log_2^{[\text{fold change}]}| \geq 1$) were set as the thresholds for significantly differential expression. Gene ontology (GO) enrichment analysis of the DEGs was implemented by the GOseq R package based on the Wallenius noncentral hypergeometric distribution (Young, Wakefield, Smyth, & Oshlack, 2010). The statistical enrichment of DEGs in Kyoto Encyclopedia of Genes and Genomes pathways was performed using KOBAS software (Mao, Cai, Olyarchuk, & Wei, 2005).

2.7 | RT-qPCR experiments

RT-qPCR experiments were conducted following our previous description (Wu et al., 2019). *BnACTIN7* was used as the internal control. The primers used in the RT-qPCR are listed in Tables S7 and S9.

2.8 | Construction of the 35S::*BnaA.GL1.a* molecular cassette and plant transformation

To generate the 35S::*BnaA.GL1.a* construct, we isolated the CDS region of *BnaA.GL1.a* using the primers listed in Table S8. The PCR fragment was cloned into a modified pCAMBIA1300 vector and driven by 35S promoter. *Agrobacterium tumefaciens* strain GV3101 carrying the sequenced construct was used to transform *gl1-1* plants by the floral dipping method. The expected transgenic seedlings survived after hygromycin treatment, and they were further confirmed by PCR experiments. Five transgenic lines were obtained, and two of them were randomly chosen for trichome observation.

2.9 | Assay of SAM sugar and auxin contents

Three hairy-leaf accessions (Nos. 741, 988 and 1081) and three glabrous-leaf accessions (Nos. 399, 987 and 1031), each with three biological replicates, were chosen for measurement of sugar and auxin contents. Auxin was extracted following the description by Zhao et al. (2015). In brief, approximately 100 mg oilseed rape SAM tissues were ground into powder with liquid nitrogen. After grinding, extraction buffer ($V_{\text{isopropanol}}:V_{\text{water}}:V_{\text{HCl}} = 2:1:0.005$) was added to the ground tissues. Indole-3-acetic-2,2-d₂ acid (Cat No. 492817, Sigma) was used as an internal standard for liquid chromatography–tandem mass spectrometry (Thermo Scientific, San Jose, CA) analysis. To measure sugar content, SAM tissues were fully ground into powder in sterile water and boiled for 20 min at 100°C. After centrifugation, the supernatant was purified with 0.25 µm Millipore filters and used for sugar content analysis in an ion chromatograph (ICS-3000, DIONEX, Germany). The machine was equipped with gold electrode, detector (PAD with Ag/AgCl) and analytical column (CarboPac PA1 [4 × 250 mm²], Thermo Scientific). After running, the column temperature was maintained at 30°C and flow rate was 1.0 ml/min. Then, 200 mM NaOH was used as eluent (Wang et al., 2019).

2.10 | Yeast two-hybrid assay

The coding regions of *BnaC.IAA3.a*, *BnaA.IAA4.a* and *BnaC.IAA17.a* were amplified and cloned into pGKBT7, and the coding regions of *BnaX.ARF18.b*, *BnaC.ARF5.a*, *BnaA.GL1.a* and *BnaC.MYB39.a* were amplified and cloned into pGADT7. Sequenced plasmids were transformed into AH109 yeast strain. Yeast two-hybrid assays were

conducted using the Yeastmaker Yeast Transformation System 2 described by Bao et al. (2019). Transformed yeast cells were incubated on SD/-Leu/-Trp and SD/-Leu/-Trp/-His media for protein interaction detection.

3 | RESULTS

3.1 | Hairy oilseed rape leaves were less attractive to starving *P. xylostella* larvae than glabrous leaves

We performed a feeding experiment to investigate the difference between glabrous and hairy leaves of oilseed rape in resisting herbivory by *P. xylostella* larvae. The glabrous and hairy leaves were collected from typical glabrous genotypes (Accession Nos. 399, 671 and 1031) and hairy genotypes (Accession Nos. 741, 988 and 1081), respectively (Table S1). In general, larger leaf areas were consumed by *P. xylostella* larvae on the glabrous leaves than on the hairy leaves (Figure S1). The total consumed area on the glabrous leaves was 40% larger than that on the hairy leaves, when the glabrous and hairy leaves were placed separately in two containers (left and middle panels of Figure S1a,b). In addition, the total consumed areas on the glabrous leaves were 100% larger than those on the hairy leaves when the glabrous and hairy leaves were arranged as alternatives in the same container (right panel of Figure S1a,c).

3.2 | The 290 core accessions represent the majority of the genetic diversity of the 991 germplasm accessions of *B. napus*

To establish an efficient population that would be easy to handle for GWAS, we selected 290 core accessions based on phylogenetic analysis and PCA. The core-accession population represents 97.3% of the SNPs and 97.9% of the indels identified in the 991-accession population (Table 1; Wu et al., 2019). A PCA plot of the first two components (PC1 and PC2) of the 991 accessions is shown in Figure 1a. The 290 red dots represent the core accessions amid the background of 991 Gy dots (Figure 1a). When based on the resequencing data of either the 290 core accessions or the 991 total accessions, the calculations of SNP distribution on the 19 chromosomes showed negligible differences (Figure 1b; Wu et al., 2019). Only minor differences in the percentages of SNPs that fall in different regions of the genome, namely, CDS, splice site donors, intergenic regions, splice site acceptors, upstream regions, splice site regions, downstream regions, introns, and intragenic regions, were observed between the two calculations (Figure 1c; Wu et al., 2019). Moreover, the differences in the rates at which the SNPs caused nonsynonymous start, synonymous coding, synonymous stop, nonsynonymous coding, start loss, stop gain, and stop loss between the two calculations were minimal (Figure 1d; Wu et al., 2019). Taken together, the 290 core accessions represent the majority of the genetic diversity of the 991-accession population.

TABLE 1 Comparison of genetic polymorphisms between the 991 accessions and the 290 core accessions that were uncovered by genome resequencing

	Worldwide collection	Core collection	Percentage (%)
Number of accessions	991	290	29.26
Number of SNPs	5,559,254	5,411,233	97.34
Number of indels	1,858,671	1,819,251	97.88
Number of SNPs for GWAS	2,753,575	2,705,480	98.25

Note: The 'percentage' column represents corresponding percentages of core-accession population in 991-accession population.

Abbreviations: GWAS, genome-wide association study; SNP, single nucleotide polymorphism.

3.3 | GWAS revealed SNPs on chromosomes A06 and C07 significantly associated with trichome development on young true leaves

We recorded the leaf trichome phenotypes at the four-true-leaf stage of the 290 core accessions at two locations, namely, Changxing (Location 1) and Zi-Jin-Gang (Location 2) (Table S1). Typical hairy and glabrous leaves were visually observed as shown in Figure 2a. On the basis of the 2,705,480 SNPs ($MAF > 0.05$, missing rate < 0.5), we performed GWAS for the trichome trait across the 290 core accessions in these two locations. In total, 424 and 421 SNP signals ($p < 10^{-6}$) were significantly associated with trichome appearance in Locations 1 and 2, respectively (Table S2). Based on these significantly associated SNP signals, we identified 288 and 176 associated genes in Locations 1 and 2, respectively (Table S3). GO enrichment results showed that the candidate genes were involved in multiple biological processes, cellular components and molecular functions (Figures S2 and S3), and the euKaryotic Orthologous Group (KOG) functions of the consensus sequences indicated that the candidate genes were mainly involved in signal transduction mechanisms (T), posttranslational modification (O), transcription (K), translation, ribosomal structure and biogenesis (J) and carbohydrate transport and metabolism (G) (Figure S4).

The Manhattan plots show that most of the significantly associated SNPs were located on Chr.A06 and Chr.C07. (Figures 2b, 4a, and 5a). The significant SNPs (from Location 1) were associated with 49 and 127 genes on Chr.A06 and Chr.C07, respectively. The significant SNPs (from location 2) were associated with 49 and 87 genes on Chr.A06 and Chr.C07, respectively (Tables S3 and S4).

3.4 | Crossover analysis between the candidates identified by GWAS and RNA-seq narrowed down the number of responsible genes

To narrow down the candidate genes identified by GWAS, we performed RNA-seq analysis to compare the differentially expressed genes (DEGs) in the SAMs of the hairy- and glabrous-leaf genotypes.

Overall, there were 324 DEGs between the hairy- and glabrous-leaf SAMs after subtracting the DEGs between accessions with the same leaf type (i.e., the hairy-leaf and glabrous-leaf types). There were 111 upregulated genes and 213 downregulated genes in the hairy-leaf SAMs relative to the glabrous-leaf SAMs (Figure 3a; Table S5). The genes were clustered on the basis of their expression level. A comparison of clusters between the three hairy-leaf and three glabrous-leaf accessions demonstrated obvious differences, which are indicated with colours in Figure 3b. The DEGs were further classified into KOG functional categories from A to Z as shown with various colours in Figure S5 and are listed with gene IDs in Table S6. The category classifications for the DEGs based on the RNA-seq analysis and for the candidate genes discovered by GWAS were quite similar in terms of gene distribution (Figures S4 and S5). Significant SNP signal peaks were detected at Chr.A06 and Chr.C07; we performed a crossover analysis between the 176 associated candidate genes on Chr.A06 and Chr.C07 identified by GWAS and the 324 DEGs revealed by RNA-seq and found seven genes that overlapped (Figure 3c). The IDs of the overlapping genes and their annotations are listed in Table 2.

3.5 | SNPs in the putative *BnaA.GL1.a*, *BnaC.SWEET4.a*, *BnaC.WAT1.a* and *BnaC.WAT1.b* genes corresponded to hairy- and glabrous-leaf divergence

Furthermore, we compared the SNPs of the seven candidate genes suggested by the crossover analysis (Table 2). The SNPs on *BnaC07g25000D* and *BnaC07g49070D* were unlikely to be responsible for the divergence of the hairy- and glabrous-leaf accessions, as there were no SNPs within the candidate genes between the two groups. There were three SNPs that locate in the fourth intron on *BnaC07g24970D* (Figure S6). Therefore, we excluded these three genes from the subsequent analysis.

BnaA06g31780D, named *BnaA.GL1.a*, is a putative ortholog of GLABRA1 (GL1), a member of the MBW trimeric activator complex that positively induces trichome formation in *Arabidopsis*. *BnaA.GL1.a* showed a much higher expression level in the hairy-leaf accessions than in the glabrous accessions, as demonstrated by RNA-seq (4.4-fold) and confirmed by RT-qPCR (7.9-fold) (Figures 4b and S7). When *gl1-1* plants were transformed with the 35S:*BnaA.GL1.a* construct, two independent T3 lines exhibited dense trichomes on the leaves and stems, indicating that *BnaA.GL1.a* could complement *gl1* in *Arabidopsis* (Figure 4c).

There were 243 SNPs on Chr.C07 that were tightly linked with each other and with *BnaC07g24860D* (*BnaC.SWEET4.a*), a putative ortholog of the bidirectional sugar transporter SWEET4 in *B. rapa* (Figure 5a,b, Tables 2 and S3). Except for one (Accession No. 617), the glabrous accessions had SNPs that were obviously different from those of the 238 hairy-leaf accessions, indicating functional and/or transcriptional differences. The SNPs between the hairy- and glabrous-leaf accessions were found not only in the 5'-end regulatory region and intron but also in the CDS (137 from the start codon), and the latter led to a change in the encoded amino acid from valine to

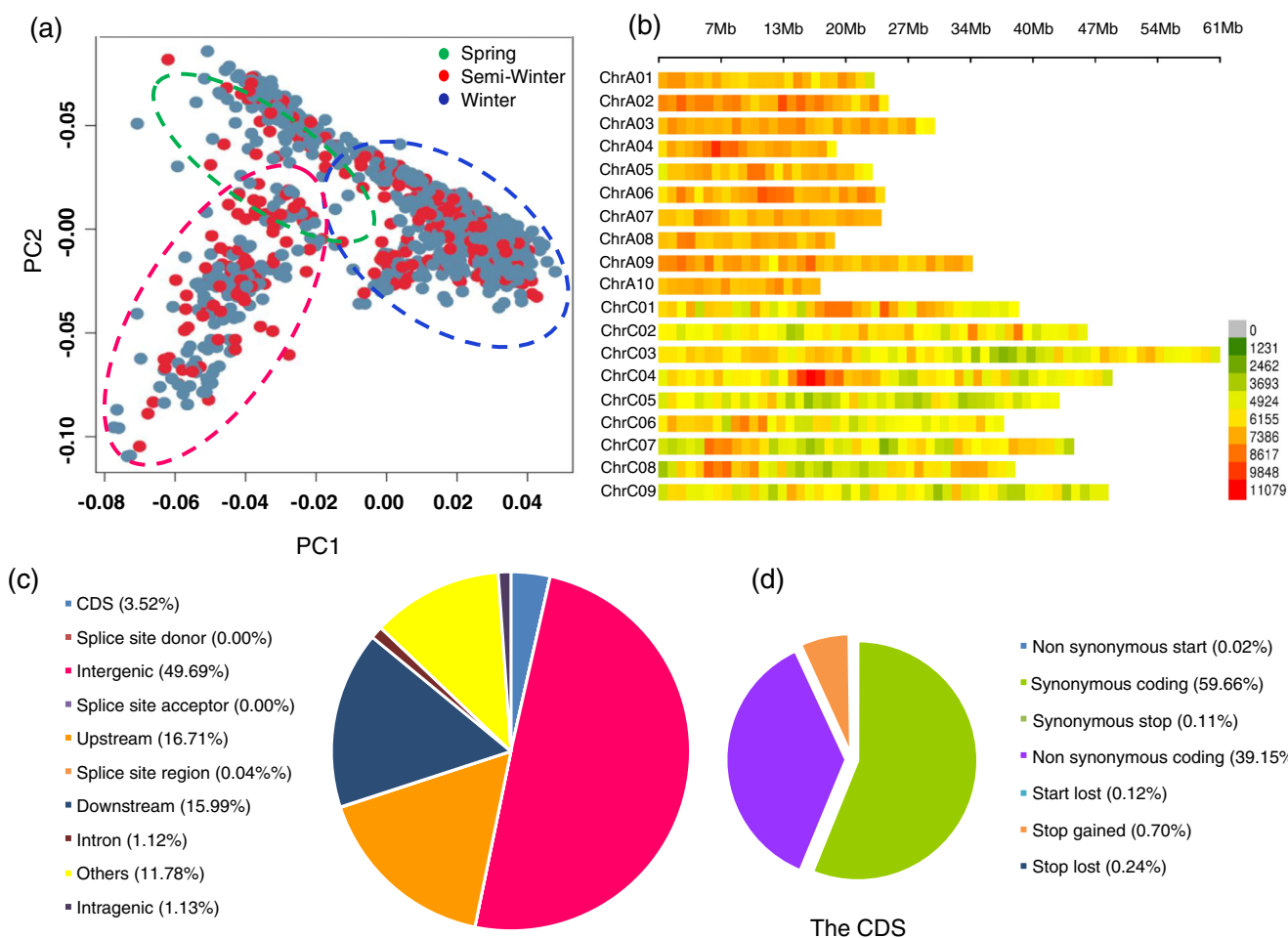


FIGURE 1 Genetic polymorphisms of the 290 core accessions revealed by genome resequencing. (a) principal component analysis (PCA) plot of two components (PC1, PC2) of a worldwide collection of 991 rapeseed germplasm accessions. PC1, indicating 11.19% of the total variation, divides the winter-type accessions from the spring-type and semiwinter accessions, whereas PC2, representing 6.90% of the total variation, separates the semiwinter types from the spring types. The 290 accessions, indicated by the red dots, derive from the 991 Gy dots. (b) Single nucleotide polymorphism (SNP) density within a 100-kb window size on the 19 chromosomes of 290 resequenced genomes. Different colours show various densities as displayed in the spectrum column. (c) Distribution of the SNPs in various genomic variations. (d) Distribution of SNPs in coding sequences (CDS) regions

aspartic acid (Figure 5c, Table 3). Furthermore, we performed single SNP association tests on the above SNPs related to *BnaC.SWEET4.a* between the hairy-leaf accessions and the glabrous accessions. We found that allele A of ChrC07_31083895 (+137) was significantly ($p < .001$) associated with the hairy-leaf trait (Table 3). *BnaC.SWEET4.a* was expressed at a much lower level in the hairy-leaf accessions than in the glabrous accessions, as demonstrated by RNA-seq (16.1-fold) (Figure S7a) and confirmed by RT-qPCR (6.9-fold) (Figure S7b).

There were 180 significant SNPs on Chr.C07 that were tightly linked with each other and with *BnaC07g24950D* (*BnaC.WAT1.a*) and *BnaC07g24960D* (*BnaC.WAT1.b*), two neighbouring genes that are putative orthologs of WALLS ARE THIN1 (WAT1) in *B. rapa* (Figure 6a, b, Tables 2 and S3). Almost all the glabrous-leaf accessions had SNP patterns in these two genes that were obviously different from those of the 238 hairy-leaf accessions, suggesting transcriptional and/or functional differences. The SNPs of *BnaC.WAT1.a* occur in the 5'-end regulatory region, introns and CDS. The SNPs in the CDS of

BnaC.WAT1.a give rise to nonsynonymous amino acid changes at positions 1902, 1921, 2031, 2082, 2,248, 2,273, 2,316, 2,703, 2,712 and 2,727 from the start codon (Figure 6c, Table 3). The SNPs of *BnaC.WAT1.b* occur in the 5'-end regulatory region, introns and CDS (the last exon). The SNPs in the CDS of *BnaC.WAT1.b* lead to non-synonymous amino acid changes at Positions 2,615 and 2,653 from the start codon (Figure 6d, Table 3). Single SNP association tests on the above SNPs related to the genes *BnaC.WAT1.a* and *BnaC.WAT1.b* between the hairy-leaf accessions and glabrous accessions were also conducted. Ten alleles, such as the A allele of ChrC07_31148683 (+1902), the A allele of ChrC07_31148702 (+1921) and the G allele of ChrC07_31149029 (+2,248) of *BnaC.WAT1.a*, were significantly correlated with hairy-leaf appearance (Figure 6c, Table 3). We found that two alleles, the C allele of ChrC07_31154625 (+2,615) and the C allele of ChrC07_31154663 (+2,653) of *BnaC.WAT1.b*, were also significantly correlated with hairy-leaf appearance (Table 3). *BnaC.WAT1.a* and *BnaC.WAT1.b*

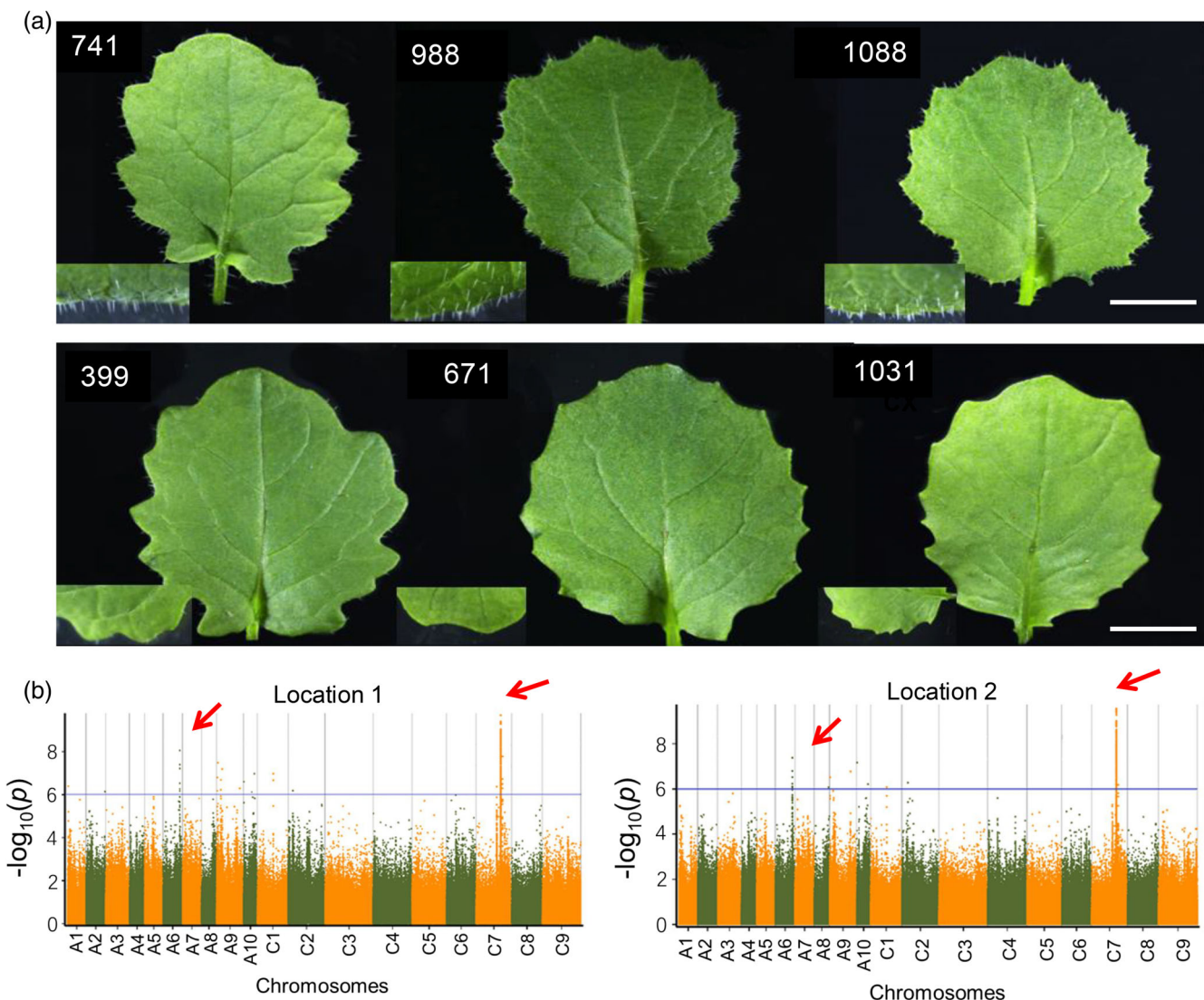


FIGURE 2 Comparison of the leaf surfaces of the H- and G-leaves and genome-wide association study (GWAS) results showing the single nucleotide polymorphisms (SNPs) associated with leaf trichome appearance at the young seedling stage. (a) Images showing typical trichomes on the leaf surface in Accession Nos. 741, 988 and 1,081 (upper panel) and the glabrous leaf surface in Accession Nos. 399, 671, and 1031 (lower panel). The magnified images left of each leaf show the hairs on the leaf margins. Bars = 1 and 0.25 cm for the intact leaves and the sections of leaf margin, respectively. (b) Manhattan plots of GWAS for Location 1 (Changxing) (left) and Location 2 (Zi-Jin-Gang Campus) (right). The SNP peaks, indicated by the red arrows, were in the regions from ~21.2 to ~21.6 Mb on Chr.A06 and from ~30.9 to ~31.2 Mb on Chr.C07, respectively. The blue line represents the significance threshold ($-\log_{10}p = 6$).

were expressed at a much lower level in the hairy-leaf accessions than in the glabrous accessions, as demonstrated by RNA-seq (Figure S7a) and confirmed by RT-qPCR (Figure S7b).

3.6 | Exogenous sugar and auxin affected trichome development on oilseed rape leaves

Because SWEET4 acts as a bidirectional sugar transporter (Jia et al., 2017; Zhang et al., 2019), and WAT1 is a vacuolar auxin transport facilitator required for intracellular auxin homeostasis in *Arabidopsis* (Ranocha et al., 2010), we suspected the role of sugar and auxin

signals in regulating leaf trichome initiation. First, we compared the glucose-, fructose-, sucrose- and indoleacetic acid (IAA) contents of the SAMs in typical hairy- and glabrous-leaf accessions. As shown in Figure 7(a), significantly higher contents of glucose and sucrose were found in the SAMs of the glabrous-leaf accessions than in those of the hairy-leaf accessions. However, there were no significant differences in fructose and IAA contents between the hairy- and glabrous-leaf accessions. Furthermore, we sprayed IAA (8 μ M) and IAA (15 μ M) and a mixture of glucose (6%) and sucrose (1%) on glabrous accessions without or with few trichomes. The IAA (8 μ M) spray significantly increased the number of trichomes on both the first and second true leaves in Accession Nos. 399 and 1048 and merely on the second

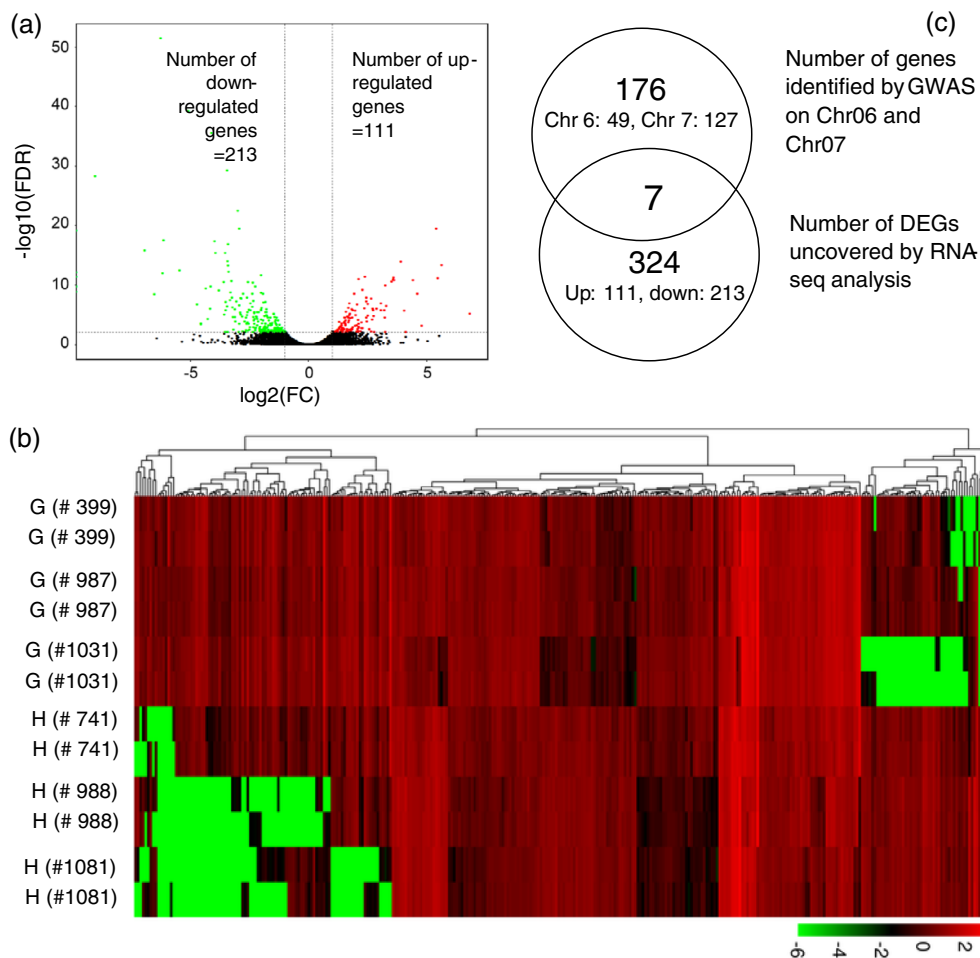


FIGURE 3 Differentially expressed genes (DEGs) in the H- and G-leaf types revealed by RNA-seq analysis. (a) Volcano plots showing the DEGs in H- and G-leaf types. The horizontal axis in $\log_2(\text{FC})$ indicates the fold changes in the expression level from the H-leaf to G-leaf type. The vertical axis represents absolute expression levels of the DEGs indicated in $-\log_{10}(\text{FDR})$ values. The black dots indicate no significant changes in gene expression between the G- and H-leaf types. The green dots represent downregulated DEGs, whereas the red dots indicate upregulated DEGs. (b) Cluster analysis of the gene expression patterns of H- and G-leaf types. Different colours show various expression levels, as displayed in the spectrum column from green (low) to red (high). Three H-leaf accessions (Nos. 741, 988 and 1,081) and three G-leaf accessions (Nos. 399, 987 and 1031) were selected for RNA-seq analysis with three biological replicates and two technical replicates each. (c) Venn diagram showing the number of candidate genes identified by genome-wide association study (GWAS), the number of genes differentially expressed in the shoot apical meristem (SAM) tissues between the H-leaf and G-leaf types and the number of overlaps

leaves in Accession Nos. 719 and 987 (Figure 7b,c). The IAA (15 μM) spray significantly increased the number of trichomes on both the first and second true leaves in Accession No. 1048. In contrast, the IAA (15 μM) spray significantly reduced the number of trichomes on both the first and second true leaves in Accession Nos. 225 and 987 (Figure 7b,c). The mixed glucose (6%) and sucrose (1%) spray reduced the number of trichomes on both the first and second leaves in all the accessions tested, but the effect was not statistically significant except on the first leaf of No. 987 (Figure 7b,c). Overall, the effects of exogenous sugar and IAA on trichome initiation depended on concentration, genotype and developmental stage. Exogenous auxin (8 μm) positively affected leaf trichome numbers in certain genotypes, whereas spraying with sucrose (1%) plus glucose (6%) slightly repressed leaf trichome development in all the genotypes tested.

3.7 | Higher expression of auxin negative regulators but lower expression of ARFs in glabrous leaves

Auxin of a proper concentration could promote trichome initiation (Figure 7b,c), but there was no significant difference in SAM auxin concentration between the hairy and glabrous accessions (Figure 7a). Thus, we next investigated the expression of negative regulators (NRs, AUX/IAA family proteins) and ARFs in the auxin signalling pathway. The transcript levels of the putative NRs in the auxin signalling pathway, such as *BnaC.IAA3.a*, *BnaA.IAA17.a*, *BnaC.IAA17.a*, and *BnaA.IAA4.a*, in the glabrous-leaf accessions were much higher than those in the hairy-leaf accessions, as revealed by RNA-seq (Figure S8) and confirmed by RT-qPCR (Figure 8c). In contrast, the transcript

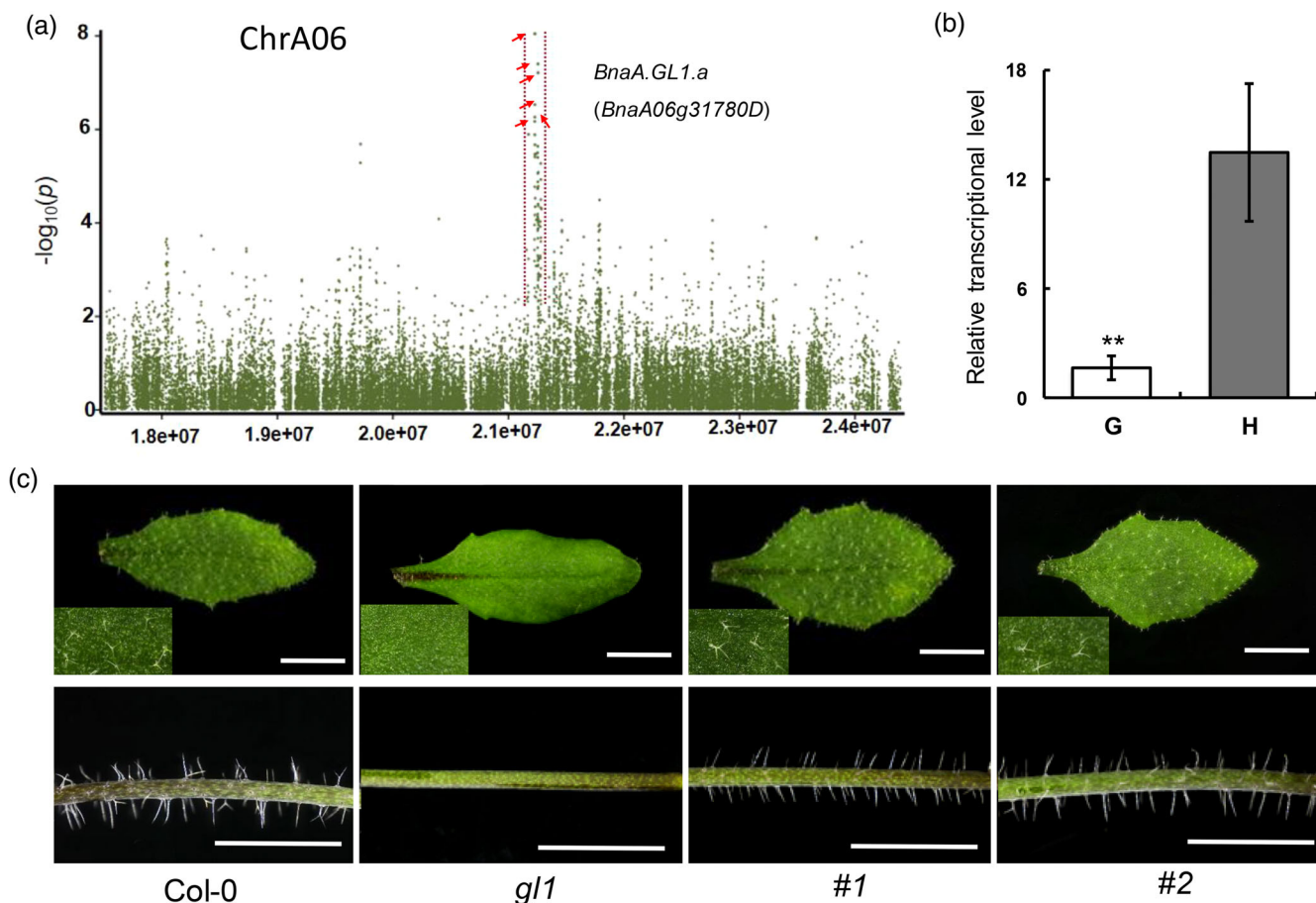


FIGURE 4 Positive regulation of *BnaA.GL1.a* on leaf trichome initiation at the young seedling stage. (a) Local Manhattan plot showing the significant single nucleotide polymorphisms (SNPs) ($-\log_{10}p > 6$) with red arrows in the *BnaA.GL1.a* (*BnaA06g31780D*) locus. All candidate genes in the region are listed and annotated in Supplementary Table S4. (b) Comparison of *BnaA.GL1.a* expression between H- and G-leaves. (c) Comparison of trichome numbers on leaves (upper panel) and stems (lower panel) between Col-0, *gl1*, and the two independent T_3 transgenic plants harbouring the 35S:*BnaA.GL1.a* complementation cassette. Bar = 4 mm. The double asterisks indicate statistically significant differences at the 1% level

levels of putative ARFs, including *BnaX.ARF18.a*, *BnaX.ARF18.b*, *BnaC.ARF5.a*, and *BnaA.ARF5.a*, were significantly lower in the glabrous-leaf accessions than in the hairy-leaf accessions (Figures 8d, S8, and S9). In addition, the putative MYB genes *BnaC.MYB39.a* and *BnGL1s*, components of the WBM complex, were upregulated in the hairy-leaf accessions (Figures 4, 8a, and S10). Auxin response elements were found in the putative *BnaC.MYB39.a* and *BnGL1* (*BnaA06g31780D* and *BnaCnng52970D*) promoters or genomic DNA regions (Figure S11). The expression levels of the *BnGL1s* and *BnaC.MYB39.a* were analysed after exogenous auxin application, and *BnaC.MYB39.a* was significantly upregulated by 8 μ M auxin (Figure 8b). In light of a previous study reporting the induction of denser trichomes by overexpression of *iaaM* that caused increased endogenous auxin synthesis in tobacco (Zhao et al., 2012), we observed 35S:*iaaM* transgenic seedlings of *Arabidopsis* (Zhang, He, Li, & Yang, 2014). In contrast to what was observed in tobacco, the 35S:*iaaM* transgenic seedlings showed significantly decreased trichome number (Figure 9a). We analysed expression levels of genes involved in MBW complex, such as the *MYB106* which is homologous with *BnaC.MYB39.a* (Figure 9b). Both WT and 35S:*iaaM*

transgenic seedlings had similar levels of *GL3* and *TTG1* expression, but the 35S:*iaaM* transgenic seedlings demonstrated downregulated levels of *GL1*, *MYB106* and *GL2* expression in comparison to the WT.

Because previous studies reported that sugar affected auxin distribution and ARF expression (Wang, Cook, Patrick, Chen, & Ruan, 2014; Yuan, Xu, Zhang, Guo, & Lu, 2014), we investigated the expression levels of *BnARF5s* and *BnARF18s* in the leaves that were treated with the sugar solution and found that the treatment reduced the expression levels of *BnARF18s* (Figure 8b).

3.8 | The interactions between *BnaC.IAA3.a*, *BnaA.IAA4.a*, *BnaC.IAA17.a* and *BnaC.ARF5.a*

In order to know which IAs and ARFs interact with each other, we performed yeast two-hybrid analysis. As shown in Figure 9c, there were no interactions between *BnARF18* and the IAs such as *BnIAA3*, *BnIAA4* and *BnIAA17*. By contrast, there were interactions between *BnaC.IAA3.a*, *BnaA.IAA4.a*, *BnaC.IAA17.a* and *BnaC.ARF5.a*.

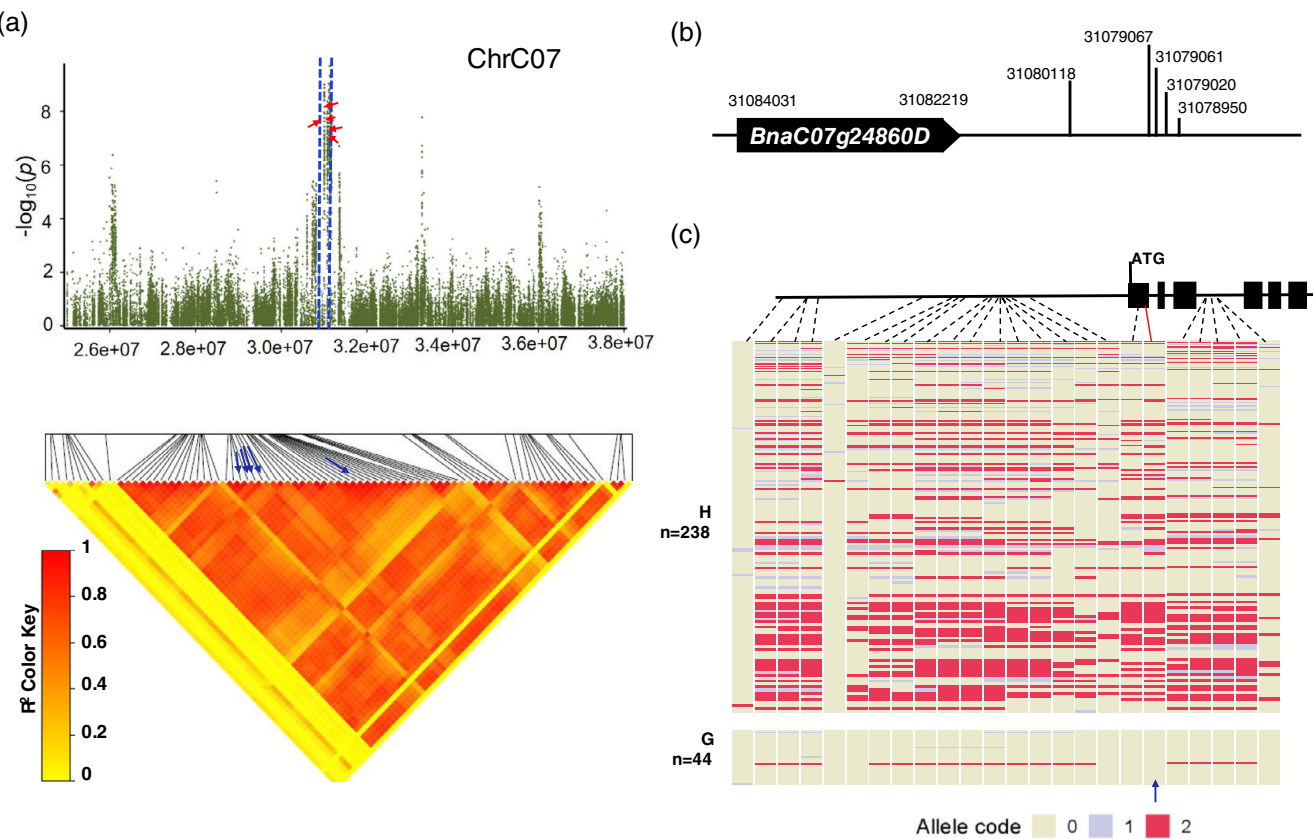


FIGURE 5 Negative regulation by *BnaC.SWEET4.a* of trichome initiation. (a) Local Manhattan plot showing a variety of single nucleotide polymorphisms (SNPs) at the peak region on Chr.C07 that are significantly ($-\log_{10}p > 6$) associated with leaf trichome formation. The arrows on the LD heat map indicate the positions of the representative SNPs (indicated by the red dots of the peak) on the heat map, which are at 31078950, 31079020, 31079061, 31079067, 31080118 on Chr.C07. The linkage degrees between each of the two positions and between the SNPs and the candidate gene *BnaC.SWEET4.a* (*BnaC07g24860D*) (from 31,084,031 to 31,082,219) are shown by the colour keys indicating r^2 values. All candidate genes of the region are listed and annotated in Supplementary Table S4. (b) A sketch magnifying the relative distance between the significant SNPs associated with leaf trichome appearance and *BnaC.SWEET4.a*. (c) A sketch showing the structure of *BnaC.SWEET4.a* and the allelic changes in *BnaC.SWEET4.a* among 286 accessions. The dashed lines indicate SNPs in regulatory sequences, and the red solid line points to the SNP leading to nonsynonymous coding between the H- and G-leaves. The SNP patterns of *BnaC.SWEET4.a* corresponded to the H- and G-leaf types, respectively

Gene ID	Regulation	Pfam_annotation	nt_annotation
BnaC07g24860D	Down	Sugar efflux transporter for intercellular exchange	<i>B. rapa</i> bidirectional sugar transporter SWEET4
BnaC07g24950D	Down	EamA-like transporter family	<i>B. rapa</i> WALLS ARE THIN1-related protein
BnaC07g24960D	Down	EamA-like transporter family	<i>B. rapa</i> WALLS ARE THIN1-related protein
BnaC07g24970D	Down	—	<i>B. rapa</i> hsp70-binding protein 1
BnaC07g25000D	Down	Glycosyltransferase like family 2	<i>B. rapa</i> xyloglucan glycosyltransferase 4
BnaC07g49070D	Up	—	<i>B. rapa</i> uncharacterized LOC103875260
BnaA06g31780D	Up	Myb-like DNA-binding domain	Trichome differentiation protein GL1 (<i>B. rapa</i>)

TABLE 2 Candidate genes narrowed down by GWAS and RNA-seq experiments and their annotations

Note: The 'down' or 'up' indicate the downregulation or upregulation of gene expression in the H-leaf accessions relative to the G-leaf accessions.

Abbreviation: GWAS, genome-wide association study.

TABLE 3 Significant SNPs in the coding regions of the putative *BnaC.SWEET4.a* (*BnaC07g24860D*), *BnaC.WAT1.a* (*BnaC07g24950D*) and *BnaC.WAT1.b* (*BnaC07g24960D*) associated with the hairy-leaf type

Locus	Associated allele	Amino acid change	Chi square	Permutation p-value	
<i>BnaC07g24860D</i>	Chr07_31083895 (+137)	A	GTT(V) GAT(D)	34.886	.0001
<i>BnaC07g24950D</i>	Chr07_31148683 (+1902)	A	CGC(R) AGC(S)	38.5	9.0000E-5
<i>BnaC07g24950D</i>	Chr07_31148702 (+1921)	A	ACT(T) AAT(N)	39.969	5.0000E-5
<i>BnaC07g24950D</i>	Chr07_31148812 (+2031)	G	CCC(P) GCC(A)	35.864	.0002
<i>BnaC07g24950D</i>	Chr07_31148863 (+2082)	G	ATA(I) GTA(V)	28.089	.001
<i>BnaC07g24950D</i>	Chr07_31149029 (+2,248)	G	ATT(I) GTT(V)	40.515	4.0000E-5
<i>BnaC07g24950D</i>	Chr07_31149054 (+2,273)	T	TCT(S) TTT(F)	36.676	.0002
<i>BnaC07g24950D</i>	Chr07_31149097 (+2,316)	G	ATT(I) ATG(M)	37.955	.0001
<i>BnaC07g24950D</i>	Chr07_31149,484 (+2,703)	G	ATT(I) GTT(V)	35.55	.0002
<i>BnaC07g24950D</i>	Chr07_31,149,493 (+2,712)	T	GAT(D) TAT(Y)	33.494	.0003
<i>BnaC07g24950D</i>	Chr07_31,149,508 (+2,727)	G	TGT(C) GGT(G)	37.023	.0002
<i>BnaC07g24960D</i>	Chr07_31154625 (+2,615)	C	GTT(V) GCT(A)	38.499	5.4781E-10
<i>BnaC07g24960D</i>	Chr07_31154663 (+2,653)	C	GTT(V) CTT(L)	29.048	7.0616E-8

Note: The case group is the H phenotype, and the control group is the G phenotype. The p-value was adjusted by the permutation test (test iterations = 100,000). In the 'Amino acid change' column, sequences of left part represents the nucleic acids of the reference genome; sequences of right part represents the nucleic acids that are changed from the reference genome. The red letters indicate the changed nucleic acids, and the letters in parentheses represent the amino acids.

4 | DISCUSSION

Leaf trichomes confer plant resistance to the diamondback moth (*P. xylostella*) in *A. thaliana* (Handley, Ekbom, & Agren, 2005) and *Arabidopsis. lyrata* (Sletvold, Huttunen, Handley, Kärkkäinen, & Ågren, 2010). In this study, we show that hairy-leaf genotypes of *B. napus* were less attractive to *P. xylostella* larvae, a pest causing tremendous damage to seedlings of Brassicaceae plants, including oilseed rape, in many parts of the world (Ahuja, Rohloff, & Bones, 2010). The resistance of the hairy leaves to this insect could arise from the physical properties of the leaf surface, which cause discomfort to the larvae, or possibly from the irritating chemicals produced by the trichomes. Gruber et al. (2018) demonstrated that transgenic hairy-leaf lines of *B. napus* expressing *Arabidopsis GL3* (*AtGL3*) led to altered flea-beetle and *P. xylostella* larvae feeding behaviour in comparison to the non-transgenic glabrous leaves of the cultivar 'Westar'. Because the cotyledons of the transgenic lines remained glabrous but also exhibited reduced insect feeding, it was concluded that not only the physical surface of the leaves but also chemical compounds such as glucosinolates, a consequence of *AtGL3* ectopic expression, conferred the resistance (Alahakoon et al., 2016; Gruber et al., 2018). Since the glucosinolate content in seeds are highly correlated with the glucosinolate content in leaves in oilseeds rape, we compared the glucosinolate content in seeds between the hairy and glabrous accessions. We did not find significant difference in glucosinolate content of the seeds between the hairy and glabrous accessions (Figure S12). Apart from flea beetles and *P. xylostella* larvae, aphids (*Brevicoryne brassicae*) also showed a preference to feed on glabrous leaves in *B. napus* (Hao, Zhan, Wang, & Hou, 2019).

In a previous study, we resequenced a worldwide collection of 991 *B. napus* germplasm accessions, and identified 5.56 million SNPs

and 1.86 million indels by mapping the reads to a reference genome ('Darmor-bzh') (Wu et al., 2019). Based on the study, here we established a core germplasm collection including only 290 accessions. Although the population is relatively small, this 290-accession core collection represents 97.3% of the SNPs and 97.9% of the indels of the 991-accession collection, representing the genetic diversity of *B. napus* of the world. In comparison with previously described GWASs, such as Arifuzzaman, Oladzadabbasabadi, McClean, and Rahman (2019), He et al. (2017), Lu et al. (2019), Wang et al. (2017) and Wu et al. (2019) and, the current approach involves a much smaller population that is easily handled for GWAS, but a very high SNP number (2705480), which lends power to the analysis and allows identification of tightly associated genes. Brassicaceae plants have a large variation in trichome formation across wild and cultivated species (Beilstein, Al-Shehbaz, & Kellogg, 2006). Our study adds insights into the ecology and evolution of leaf trichome variation in the species *B. napus*.

We identified 49 and 127 neighbouring genes that were significantly correlated with the 6 and 272 significant SNPs on Chr.A06 and Chr.C07, respectively (Tables S2–S4). To narrow down the candidates, we applied RNA-seq analysis to compare the DEGs between hairy- and glabrous-leaf SAMs. There were 111 upregulated and 213 downregulated genes in the hairy-leaf SAMs relative to the glabrous-leaf SAMs (Figure 3a,c). A larger number of downregulated genes in the hairy-leaf accessions might arise from the fact that the hairy-leaf SAMs had 3.9-fold lower expression of a putative TATA-binding protein associated factor 5 (TAF5) (*BnaA08g00370D*) than the glabrous-leaf SAMs (Figure S7a), as TAFs are required for the initiation of transcription mediated by RNA polymerase II (Albright & Tjian, 2000; Lago, Clerici, Mizzi, Colombo, & Kater, 2004).

GLABRA1 (*GL1*), a R2R3 MYB-related transcriptional factor, participates in the MBW trimeric activator complex positively regulating

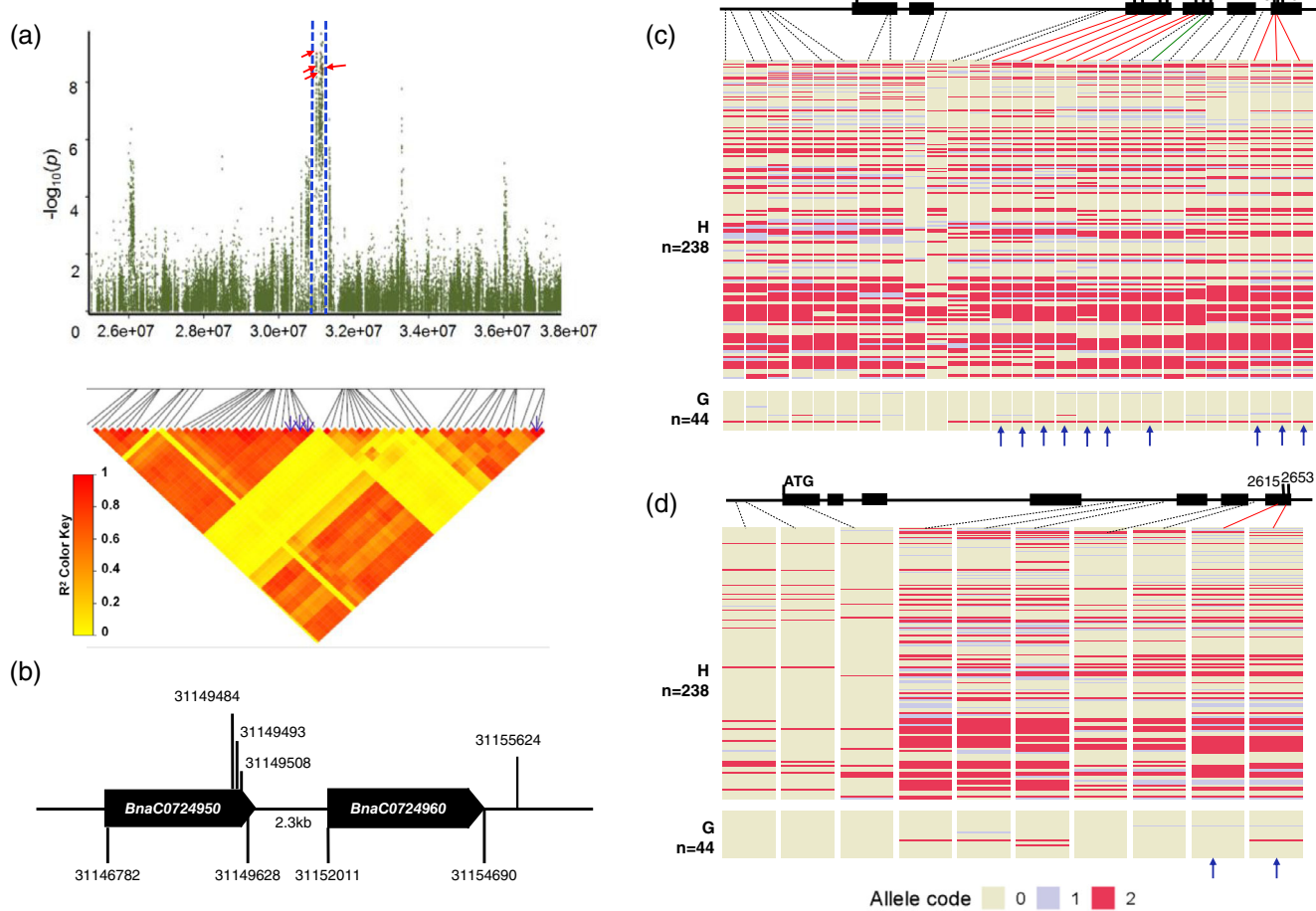


FIGURE 6 Negative regulation by *BnaC.WAT1.a* (*BnaC07g24950D*) and *BnaC.WAT1.b* (*BnaC07g24960D*) of leaf trichome initiation. (a) Local Manhattan plot showing the significant single nucleotide polymorphisms (SNPs) at the peak region on Chr.C07 that are associated with leaf trichome formation ($-\log_{10}p > 6$). The arrows in blue indicate the positions of the representative SNPs on the heat map, which are at 31149484, 31149493, 31,149,508, 31,155,624 on Chr.C07. The linkage degrees between each of the two positions and between the SNPs and the candidate genes *BnaC.WAT1.a* from 31,146,782 to 3,149,628 and *BnaC.WAT1.b* from 31,152,011 to 31,154,690 are reflected by the colour keys indicating r^2 values. (b) A sketch showing the positions of *BnaC.WAT1.a*, *BnaC.WAT1.b* and the significant SNPs linked with these two genes. (c) A sketch showing the structure of *BnaC.WAT1.a* and the SNPs in the 5'-end regulatory region and the exon and intron regions of the gene. (d) A sketch showing the structure of *BnaC.WAT1.b* and the SNPs in the 5'-end regulatory region and the exon and intron regions of the gene. In (c) and (d), the dashed lines indicate SNPs in the regulatory sequence, and the red solid lines indicate the SNPs in the coding sequences leading to nonsynonymous amino acid changes. The patterns of SNPs in the regulatory region and coding region of *BnaC.WAT1.b* clearly distinguished the H-leaf type from the G-leaf type

trichome development in *Arabidopsis* (Kirik, 2005; Pattanaik, Patra, Singh, & Yuan, 2014; Szymanski & Marks, 1998; Tominaga-Wada et al., 2012). The *gl1* loss-of-function mutants are well known in natural accessions of *A. thaliana* (Bloomer, Juenger, & Symonds, 2012; Hauser, Harr, & Schlätterer, 2001), *A. lyrata* (Kivimäki, Kärkkäinen, Gaudeul, Loe, & Ågren, 2007) and *A. halleri* (Kawagoe, Shimizu, Kakutani, & Kudoh, 2011). *BnaA06g31780D* (*BnaA.GL1.a*) is a putative ortholog of *AtGL1*. We demonstrated that the *gl1-1* *Arabidopsis* plants harbouring the 35S:*BnaA.GL1.a* cassette developed trichomes on the leaves and stems, indicating that *B. napus* might share a similar regulatory network with *Arabidopsis* for the control of trichome development (Figure 4c). The MBW-regulatory network for trichome (or hair) development could be similar in various developmental processes in different plants, for example, seed hair (fibre) development in cotton

is also mediated by the MBW complex. *Gossypium arboreum* *MYB2* (*GaMYB2*), which encodes a putative ortholog of *GL1*, complemented the hairless *gl1* mutant and resulted in occasional hair formation on *Arabidopsis* seeds (Wang et al., 2004). *BnaC.MYB39.a* shows higher expression level in hairy Brassica seedlings. Overexpression of *PtaMYB186*, which is orthologous to *BnaC.MYB39.a*, results in fuzzy leaf in *Populus* (Plett et al., 2010). Therefore, *BnGL1* and *BnMYB39* positively regulate trichome formation.

BnaC07g24950D and *BnaC07g24960D* (*BnaC.WAT1.a* and *BnaC.WAT1.b*) are putative orthologs of *Arabidopsis WAT1*, which is a vacuolar auxin transport facilitator required for auxin homeostasis (Ranocha et al., 2010). Auxin plays a crucial role in many aspects of plant growth, from controlling branches and root architecture, abiotic and biotic stress responses and directional growth responses to

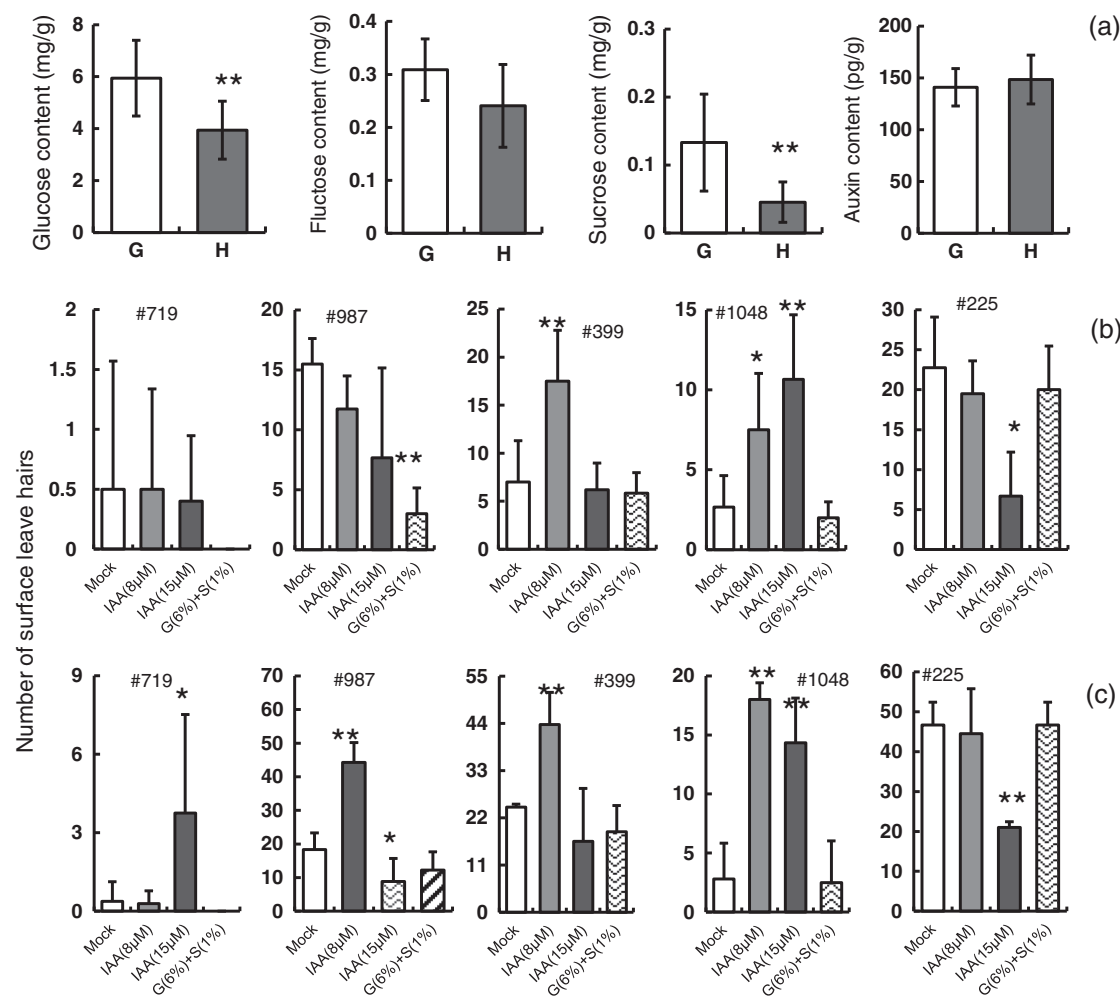


FIGURE 7 The effects of sugar and auxin on trichome initiation. (a) Comparison of sugar (glucose, fructose and sucrose) and auxin contents between the shoot apical meristems (SAMs) of the H- (Nos. 741, 988 and 1081) and G-leaf (Nos. 399, 987 and 1031) accessions. (b) The effect of exogenous sugar and auxin application on trichome formation on the first true leaves of the glabrous accessions. (c) The effect of exogenous sugar and auxin application on trichome formation on the second true leaves of the glabrous accessions. The error bars represent the standard variations. Single and double asterisks (*) indicate statistical significance to the control at $p \leq .01$ and $p \leq .05$ levels, respectively

impacting reproductive development (Vanneste & Friml, 2009; Wang et al., 2005; Zhang et al., 2011). We report here that auxin signalling plays a role in inducing trichome initiation on the leaves of *B. napus*. Although there was no significant difference in SAM auxin concentration between the hairy-leaf and glabrous-leaf accessions, the lower expression of NRs in the auxin signalling pathway, namely, the putative *BnaC.IAA3.a*, *BnaA.IAA4.a*, *BnaC.IAA17.a*, should lead to higher expression of *BnaC.AR5.a*, as evidence of yeast two-hybrid assay revealed the interactions between the NRs and the ARF (Figures 8, 9 and S8). GL1 interacts with DELLA and JAZ proteins to regulate trichome formation (Chini et al., 2007; Qi et al., 2014). We performed Y2H to detect if *BnGL1* and *BnMYB39* interact with IAA proteins, and the results were negative (Figure 9c). Auxin and GA regulate trichome formation in different pathways.

In this study, we showed that specific auxin concentrations promoted trichome initiation, while high auxin level inhibited trichome formation (Figure 7). This phenomenon also exists in various plant species, for example, overexpression of *iaaM* gene leads to denser

trichomes in tobacco but reduced trichomes in *Arabidopsis* (Figure 9; Zhao et al., 2012). Because auxin responsive elements were found in the promoter region of *35S:BnaA.GL1.a* and *BnaC.MYB39.a*, we analysed the expression of *35S:BnaA.GL1.a* and *BnaC.MYB39.a*. *BnaC.MYB39.a* was considerably upregulated in response to exogenous auxin application (Figures 8b and S11). Moreover, the comparison of expression levels of *AtGL1* and *AtMYB106* (orthologous to *BnaC.MYB39.a*) between Col-0 and *35S:iaaM* transgenic seedlings (Figure 9b) revealed that *AtGL1* and *AtMYB106* were significantly down-regulated in the *35S:iaaM* transgenic seedlings. In the auxin signalling pathway, AUX/IAAs proteins interact with ARFs, and ARFs further act as either activators or inhibitors of the downstream auxin responsive genes (Dharmasiri & Estelle, 2004). *BnaA.GL1.a* and *BnaC.MYB39.a* could be possible targets of *BnaC.AR5.a*. The role of GA in regulating trichome formation was also reported (Qi et al., 2014). Auxin can induce GA biosynthesis and enhance GA signalling by destabilizing GA-mediated DELLA protein (Frigerio et al., 2006; Fu & Harberd, 2003). Both RGA and RGL2, two important members of the

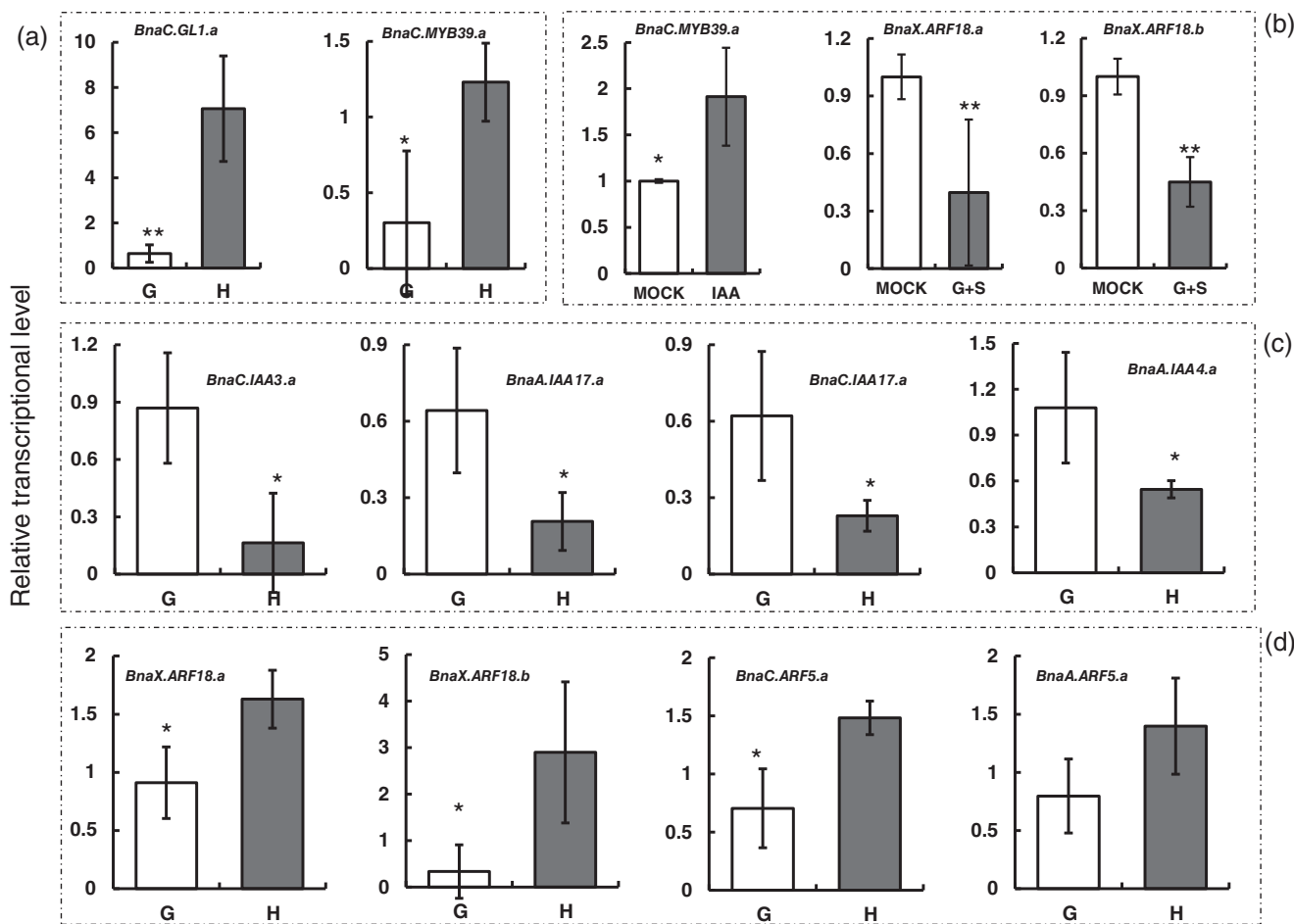


FIGURE 8 Comparison of the expression levels of putative genes in the auxin signalling pathway between the H- and G-leaf types and between mock-treated seedlings and seedlings treated with exogenous auxin or sugars. (a) Comparison of the putative *BnaC,GL1.a* and *BnaC,MYB39.a* expression between G- and H-leaf types by real-time quantitative PCR (RT-qPCR). (b) Comparison of the expression of *BnaC,MYB39.a*, *BnaX,ARF18.a*, *BnaX,ARF18.b* between the mock-treated seedlings and the seedlings treated with IAA (8 µM) and sugars (glucose [6%] + sucrose [1%]). (c) Comparison of the expression of putative negative regulators (upper panel) and putative auxin responsive factors between the G- and H-leaf types. The values of the bars are the means of three biological replicates. The error bars represent the standard variations. Single and double asterisks (*) indicate statistical significance relative to the control at $p \leq .01$ and $p \leq .05$ levels, respectively. *BnaACTIN7* was used as an internal standard in the RT-qPCR experiments

DELLA family, inhibit the transcriptional function of GL1 and GL3 (Qi et al., 2014). However, merely AtGL1 and not AtGL3, was specifically upregulated in the 35S: iaaM transgenic lines where the biosynthesis of auxin was increased (Figure 9b). Therefore, auxin may regulate trichome formation through other pathways which are independent of DELLA proteins (Fu & Harberd, 2003).

BnaC07g24860D (*BnaC,SWEET4.a*) is a putative ortholog of *Medicago truncatula* NODULIN3, a sugar efflux transporter for intercellular exchange. SWEET4 plays a critical role in mediating sugar supply to axial tissues, and the tight control of SWEET4 expression is pivotal for axial development in Arabidopsis (Liu et al., 2016). Sugar signalling, in particular GhVIN1-derived hexose signalling, plays an indispensable role in cotton (*Gossypium hirsutum*) fibre initiation by regulating the transcription of several MYB TFs and auxin signalling components that are required for fibre development (Wang et al., 2014). In contrast to the positive effect of hexose signalling on cotton seed hair initiation, we demonstrated a negative effect of sugar on trichome

development in oilseed rape leaves. Sugar signalling may crosstalk with auxin signalling by repressing the expression of some ARFs, such as ARF18, and subsequently exert impacts on leaf trichome initiation (Figure 8b; Moore, 2003; Mishra, Singh, Aggrawal, & Laxmi, 2009; Yuan et al., 2014).

GWAS is an efficient strategy to identify functional genes controlling agronomic or quality traits. In this study, we highlighted the roles of *BnaA06g31780D* (*BnaC,GL1.a*), *BnaC07g24860D* (*BnaC,SWEET4.a*), *BnaC07g24950D* (*BnaC,WAT1.a*), and *BnaC07g24960D* (*BnaC,WAT1.b*) in leaf trichome development in *B. napus*, which is a typical allotetraploid consisting of two subgenomes. In parallel to a single Arabidopsis gene, 2–10 orthologous copies normally exist in *B. napus*, which are by no means all functional. Many factors, such as the stringency of SNP calling, the environmental conditions, the method of phenotyping, and the size, diversity and structure of the population would affect GWAS results. Our study shows that appropriate auxin concentrations could positively affect trichome development by

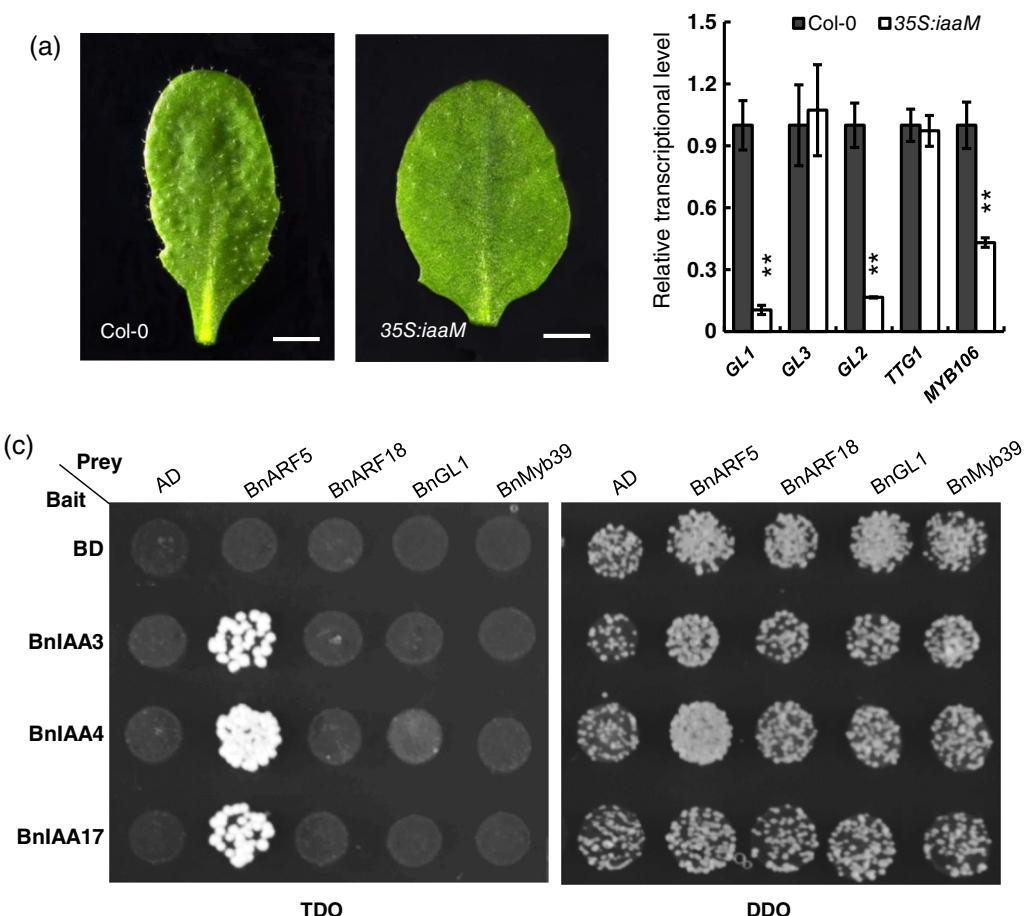


FIGURE 9 The regulation of auxin on genes involved in trichome formation. (a) Comparison of trichome (leaf hair) distribution between Col-0 and the transgenic line harbouring the 35S:iaaM construct with elevated auxin synthesis level. Bar = 1 cm. (b) Comparison of genes expression level between Col-0 and 35S:iaaM transgenic leaves. Single and double asterisks (*) indicate statistical significance relative to the control at $p \leq 0.01$ and $p \leq 0.05$ levels, respectively. The β -tubulin gene (*TUB2*) was used as an internal standard in the real-time quantitative PCR (RT-qPCR) experiments. (c) Yeast two-hybrid assay showed the protein interactions between BnaC.IAA3.a, BnaA.IAA4.a, BnaC.IAA17.a and BnaC.ARF5.a. Transformed yeast cells were incubated on SD/-Leu/-Trp (right lane) and SD/-Leu/-Trp/-His plus 5 mM 3-AT (left lane) media for protein interaction detection

downregulating NRs such as *BnaC.IAA3.a*, *BnaA.IAA4.a*, and *BnaC.IAA17.a* in the auxin signalling pathway, leading to higher expression of *BnaCARF5.a*. Sugar signalling could crosstalk with auxin signalling, affecting trichome development by inhibiting the expression of *BnARF18s*. Overall, we provide evidence indicating a new role for auxin in regulating leaf trichome development in oilseed rape.

ACKNOWLEDGEMENTS

The authors thank Prof Hongquan Yang for generously sharing the 35S:iaaM seeds, and the Institute of Entomology of Zhejiang University for providing the *P. xylostella* larvae in the feeding experiment. The work was sponsored by Natural Science Foundation of China (No. 31671597), the National Key Basic Research Project (No. 2015CB150205), Fundamental Research Funds for the Central Universities (2019FZA6011), and Jiangsu Collaborative Innovation Centre for Modern Crop Production, and the 111 project for introduction of foreign experts (B17039).

ORCID

Dezhi Wu <https://orcid.org/0000-0002-7900-0542>

Lixi Jiang <https://orcid.org/0000-0002-8579-0763>

REFERENCES

- Ahuja, I., Rohloff, J., & Bones, A. M. (2010). Defence mechanisms of Brassicaceae: Implications for plant-insect interactions and potential for integrated pest management. *Agronomy for Sustainable Development*, 30, 311–348.
- Alahakoon, U. I., Taheri, A., Nayudu, N. K., Epp, D., Yu, M., Parkin, I., ... Gruber, M. Y. (2016). Hairy canola (*Brassica napus*) re-visited: Down-regulating TTG1 in an AtGL3-enhanced hairy leaf background improves growth, leaf trichome coverage, and metabolite gene expression diversity. *BMC Plant Biology*, 16, 12.
- Albright, S. R., & Tjian, R. (2000). TAFs revisited: More data reveal new twists and confirm old ideas. *Gene*, 242, 1–13.
- Arifuzzaman, M., Oladzadabbasabadi, A., McClean, P., & Rahman, M. (2019). Shovelomics for phenotyping root architectural traits of rapeseed/canola (*Brassica napus* L.) and genome-wide association mapping. *Molecular Genetics and Genomics*, 294(4), 985–1000.

- Bao, S. J., Hua, C. M., Huang, G. Q., Cheng, P., Gong, X. M., Shen, L. S., & Yu, H. (2019). Molecular basis of natural variation in photoperiodic flowering responses. *Developmental Cell*, 50, 1–12.
- Barrett, J. C., Fry, B., Maller, J., & Daly, M. J. (2005). Haploview: Analysis and visualization of LD and haplotype maps. *Bioinformatics*, 21, 263–265.
- Beilstein, M. A., Al-Shehbaz, I. A., & Kellogg, E. A. (2006). Brassicaceae phylogeny and trichome evolution. *American Journal of Botany*, 93(4), 607–619.
- Benz, B. W., & Martin, C. E. (2006). Foliar trichomes, boundary layers, and gas exchange in 12 species of epiphytic Tillandsia (Bromeliaceae). *Journal of Plant Physiology*, 163, 648–656.
- Bloomer, R. H., Juenger, T. E., & Symonds, V. V. (2012). Natural variation in GL1 and its effects on trichome density in *Arabidopsis thaliana*. *Molecular Ecology*, 21(14), 3501–3515.
- Bradbury, P. J., Zhang, Z., Kroon, D. E., Casstevens, T. M., Ramdoss, Y., & Buckler, E. S. (2007). TASSEL: Software for association mapping of complex traits in diverse samples. *Bioinformatics*, 23, 2633–2635.
- Chalhoub, B., Denoeud, F., Liu, S., Parkin, I. A. P., Tang, H., Wang, X., ... Wincker, P. (2014). Early allopolyploid evolution in the post-Neolithic *Brassica napus* oilseed genome. *Science*, 345, 950–953.
- Chini, A., Fonseca, S., Fernández, G., Adie, B., Chico, J. M., Lorenzo, O., ... Solano, R. (2007). The JAZ family of repressors is the missing link in jasmonate signalling. *Nature*, 448, 666–671.
- Dharmasiri, N., & Estelle, M. (2004). Auxin signaling and regulated protein degradation. *Trends in Plant Science*, 9, 302–308.
- Du, X., Huang, G., He, S., Yang, Z., Sun, G., Ma, X., ... Li, F. (2018). Resequencing of 243 diploid cotton accessions based on an updated A genome identifies the genetic basis of key agronomic traits. *Nature Genetics*, 50, 796–802.
- Ehleringer, J., Bjorkman, O., & Mooney, H. A. (1976). Leaf pubescence: Effects on absorptance and photosynthesis in a desert shrub. *Science*, 192, 376–377.
- Frigerio, M., Alabadí, D., Pérez-Gómez, G., García-Cárcel, L., Phillips, A. L., Hedden, P., ... Blázquez, M. A. (2006). Transcriptional regulation of gibberellin metabolism genes by auxin signaling in *Arabidopsis*. *Plant Physiology*, 142, 553–563.
- Fu, X., & Harberd, N. P. (2003). Auxin promotes *Arabidopsis* root growth by modulating gibberellin response. *Nature*, 421(6924), 740–743.
- Gruber, M., Alahakoon, U., Taheri, A., Nagubushana, N., Zhou, R., Aung, B., ... Hegedus, D. D. D. (2018). The biochemical composition and transcriptome of cotyledons from *Brassica napus* lines expressing the AtGL3 transcription factor and exhibiting reduced flea beetle feeding. *BMC Plant Biology*, 18, 64.
- Handley, R., Ekbom, B., & Agren, J. (2005). Variation in trichome density and resistance against a specialist insect herbivore in natural populations of *Arabidopsis thaliana*. *Ecological Entomology*, 30(3), 284–292.
- Hao, Z. P., Zhan, H. X., Wang, Y. L., & Hou, S. M. (2019). How cabbage Aphids *Brevicoryne brassicae* (L.) make a choice to feed on *Brassica napus* cultivars. *Insects*, 10(3), 75.
- Hauser, M. T. (2014). Molecular basis of natural variation and environmental control of trichome patterning. *Frontiers in Plant Science*, 5, 320.
- Hauser, M. T., Harr, B., & Schlötterer, C. (2001). Trichome distribution in *Arabidopsis thaliana* and its close relative *Arabidopsis lyrata*: Molecular analysis of the candidate gene GLABROUS1. *Molecular Biology and Evolution*, 18(9), 1754–1763.
- He, Y., Wu, D., Wei, D., Fu, Y., Cui, Y., Dong, H., ... Qian, W. (2017). GWAS, QTL mapping and gene expression analyses in *Brassica napus* reveal genetic control of branching morphogenesis. *Scientific Reports*, 7, 15971.
- Jameson, H. R. (1960). γ -BHC liquid seed dressing for the control of turnip flea beetle. *Journal of the Science of Food and Agriculture*, 11(9), 528–534.
- Jia, B., Zhu, X. F., Pu, Z. J., Duan, Y. X., Hao, L. J., Zhang, J., ... Xuan, Y. H. (2017). Integrative view of the diversity and evolution of SWEET and SemiSWEET sugar transporters. *Frontiers in Plant Science*, 8, 2178.
- Kawagoe, T., Shimizu, K. K., Kakutani, T., & Kudoh, H. (2011). Coexistence of trichome variation in a natural plant population: A combined study using ecological and candidate gene approaches. *PLoS One*, 6(7), e22184.
- Khanzada, K. A., Rajput, M. A., Shah, G. S., Lodhi, A. M., & Mehboob, F. (2002). Effect of seed dressing fungicides for the control of seedborne mycoflora of wheat. *Asian Journal of Plant Sciences*, 1, 441–444.
- Kim, D., Langmead, B., & Salzberg, S. L. (2015). HISAT: A fast spliced aligner with low memory requirements. *Nature Methods*, 12, 357–360.
- Kirik, V. (2005). Functional diversification of MYB23 and GL1 genes in trichome morphogenesis and initiation. *Development*, 132, 1477–1485.
- Kivimäki, M., Kärkkäinen, K., Gaudreul, M., Løe, G., & Ågren, J. (2007). Gene, phenotype and function: GLABROUS1 and resistance to herbivory in natural populations of *Arabidopsis lyrata*. *Molecular Ecology*, 16(2), 453–462.
- Koudounas, K., Manioudaki, M. E., Kourtzi, A., Banilas, G., & Hatzopoulos, P. (2015). Transcriptional profiling unravels potential metabolic activities of the olive leaf non-glandular trichome. *Frontiers in Plant Science*, 6, 633.
- Lago, C., Clerici, E., Mizzi, L., Colombo, L., & Kater, M. M. (2004). TBP-associated factors in *Arabidopsis*. *Gene*, 342, 231–241.
- Laxmi, A., Paul, L. K., Peters, J. L., & Khurana, J. P. (2004). *Arabidopsis* constitutive photomorphogenic mutant, bls1, displays altered brassinosteroid response and sugar sensitivity. *Plant Molecular Biology*, 56, 185–201.
- Lescot, M., Déhais, P., Thijs, G., Marchal, K., Moreau, Y., Van de Peer, Y., ... Rombauts, S. (2002). PlantCARE, a database of plant cis-acting regulatory elements and a portal to tools for in silico analysis of promoter sequences. *Nucleic Acids Research*, 30, 325–327.
- Liu, X., Zhang, Y., Yang, C., Tian, Z., & Li, J. (2016). AtSWEET4, a hexose facilitator, mediates sugar transport to axial sinks and affects plant development. *Scientific Reports*, 6, 24563.
- Love, M. I., Huber, W., & Anders, S. (2014). Moderated estimation of fold change and dispersion for RNA-seq data with DESeq2. *Genome Biology*, 15, 550.
- Lu, K., Wei, L., Li, X., Wang, Y., Wu, J., Liu, M., ... Li, J. (2019). Whole-genome resequencing reveals *Brassica napus* origin and genetic loci involved in its improvement. *Nature Communications*, 10, 1154.
- Mao, X., Cai, T., Olyarchuk, J. G., & Wei, L. (2005). Automated genome annotation and pathway identification using the KEGG Orthology (KO) as a controlled vocabulary. *Bioinformatics*, 21, 3787–3793.
- Mishra, B. S., Singh, M., Aggrawal, P., & Laxmi, A. (2009). Glucose and auxin signaling interaction in controlling *Arabidopsis thaliana* seedlings Root growth and development. *PLoS One*, 4, e4502.
- Moore, B. (2003). Role of the *Arabidopsis* glucose sensor HXK1 in nutrient, light, and hormonal signaling. *Science*, 300, 332–336.
- Novak, S. D., & Whitehouse, G. A. (2013). Auxin regulates first leaf development and promotes the formation of protocorm trichomes and rhizome-like structures in developing seedlings of *Spathoglottis plicata* (Orchidaceae). *AoB Plants*, 5, pls053.
- Oppenheimer, D. G., Herman, P. L., Sivakumaran, S., Esch, J., & Marks, M. D. (1991). A myb gene required for leaf trichome differentiation in *Arabidopsis* is expressed in stipules. *Cell*, 67, 483–493.
- Pattanaik, S., Patra, B., Singh, S. K., & Yuan, L. (2014). An overview of the gene regulatory network controlling trichome development in the model plant, *Arabidopsis*. *Frontiers in Plant Science*, 5, 259.
- Payne, C. T., Zhang, F., & Lloyd, A. M. (2000). GL3 encodes a bHLH protein that regulates trichome development in *Arabidopsis* through interaction with GL1 and TTG1. *Genetics*, 156, 1349–1362.
- Plett, J. M., Wilkins, O., Campbell, M. M., Ralph, S. G., & Regan, S. (2010). Endogenous overexpression of *Populus* MYB186 increases trichome density, improves insect pest resistance, and impacts plant growth: Poplar MYB186 impacts growth and pest resistance. *The Plant Journal*, 64, 419–432.
- Purcell, S., Neale, B., Todd-Brown, K., Thomas, L., Ferreira, M. A. R., Bender, D., ... Sham, P. C. (2007). PLINK: A toolset for whole-genome

- association and population-based linkage analysis. *American Journal of Human Genetics*, 81, 559–575.
- Qi, T., Huang, H., Wu, D., Yan, J., Qi, Y., Song, S., & Xie, D. (2014). Arabidopsis DELLA and JAZ proteins bind the WD-repeat/bHLH/MYB complex to modulate gibberellin and jasmonate signaling synergy. *The Plant Cell*, 26, 1118–1133.
- Ranocha, P., Denancé, N., Vanholme, R., Freydier, A., Martinez, Y., Hoffmann, L., ... Goffner, D. (2010). Walls are thin 1 (WAT1), an Arabidopsis homolog of *Medicago truncatula* NODULIN21, is a tonoplast-localized protein required for secondary wall formation in fibers: Tonoplastic WAT1 and secondary wall formation. *The Plant Journal*, 63, 469–483.
- Schellmann, S., & Hulskamp, M. (2005). Epidermal differentiation: Trichomes in *Arabidopsis* as a model system. *The International Journal of Developmental Biology*, 49, 579–584.
- Slatkin, M. (2008). Linkage disequilibrium—understanding the evolutionary past and mapping the medical future. *Nature Reviews. Genetics*, 9, 477–485.
- Sletvold, N., Huttunen, P., Handley, R., Kärkkäinen, K., & Ågren, J. (2010). Cost of trichome production and resistance to a specialist insect herbivore in *Arabidopsis lyrata*. *Evolutionary Ecology*, 24(6), 1307–1319.
- Stefanowicz, K., Lannoo, N., Zhao, Y., Eggermont, L., Van Hove, J., Al, A. B., & Van Damme, E. J. M. (2016). Glycan-binding F-box protein from *Arabidopsis thaliana* protects plants from pseudomonas syringae infection. *BMC Plant Biology*, 16, 213.
- Szymanski, D. B., & Marks, M. D. (1998). GLABROUS1 overexpression and TRITYCHON alter the cell cycle and trichome cell fate in *Arabidopsis*. *The Plant Cell*, 17(10), 2047–2062.
- Tominaga-Wada, R., Nukumizu, Y., Sato, S., Kato, T., Tabata, S., & Wada, T. (2012). Functional divergence of MYB-related genes, WEREWOLF and AtMYB23 in *Arabidopsis*. *Bioscience, Biotechnology, and Biochemistry*, 76, 883–887.
- Vanneste, S., & Friml, J. (2009). Auxin: A trigger for change in plant development. *Cell*, 136, 1005–1016.
- Walker, A. R., Davison, P. A., Bolognesi-Winfield, A. C., James, C. M., Srinivasan, N., Blundell, T. L., ... Gray, J. C. (1999). The TRANSPARENT TESTA GLABRA1 locus, which regulates trichome differentiation and anthocyanin biosynthesis in *Arabidopsis*, encodes a WD40 repeat protein. *The Plant Cell*, 11, 1337–1350.
- Wang, J., Xian, X., Xu, X., Qu, C., Lu, K., Li, J., & Liu, L. (2017). Genome-wide association mapping of seed coat color in *Brassica napus*. *Journal of Agricultural and Food Chemistry*, 65, 5229–5237.
- Wang, J. W., Wang, L. J., Mao, Y. B., Cai, W. J., Xue, H. W., & Chen, X. Y. (2005). Control of root cap formation by MicroRNA-targeted auxin response factors in *Arabidopsis*. *The Plant Cell*, 17, 2204–2216.
- Wang, L., Cook, A., Patrick, J. W., Chen, X. Y., & Ruan, Y. L. (2014). Silencing the vacuolar invertase gene GhVIN1 blocks cotton fiber initiation from the ovule epidermis, probably by suppressing a cohort of regulatory genes via sugar signaling. *The Plant Journal*, 78, 686–696.
- Wang, S., Wang, J. W., Yu, N., Li, C. H., Luo, B., Gou, J. Y., ... Chen, X. Y. (2004). Control of plant trichome development by a cotton fiber MYB gene. *The Plant Cell*, 16, 2323–2334.
- Wang, S. D., Yokosho, K., Guo, R. Z., Whelan, J., Ruan, Y. L., Ma, J. F., & Shou, H. X. (2019). The soybean sugar transporter GmSWEET15 mediates sucrose export from endosperm to early embryo. *Plant Physiology*, 180, 2133–2141.
- Wei, D., Cui, Y., He, Y., Xiong, Q., Qian, L., Tong, C., ... Qian, W. (2017). A genome-wide survey with different rapeseed ecotypes uncovers footprints of domestication and breeding. *Journal of Experimental Botany*, 68, 4791–4801.
- Wu, D., Liang, Z., Yan, T., Xu, Y., Xuan, L., Tang, J., ... Jiang, L. (2019). Whole-genome resequencing of a worldwide collection of rapeseed accessions reveals the genetic basis of ecotype divergence. *Molecular Plant*, 12, 30–43.
- Young, M. D., Wakefield, M. J., Smyth, G. K., & Oshlack, A. (2010). Gene ontology analysis for RNA-seq: Accounting for selection bias. *Genome Biology*, 11, R14.
- Yuan, T. T., Xu, H. H., Zhang, K. X., Guo, T. T., & Lu, Y. T. (2014). Glucose inhibits root meristem growth via ABA INSENSITIVE 5, which represses PIN1 accumulation and auxin activity in *Arabidopsis*: Glucose causes root defects via ABI5 and auxin signaling. *Plant, Cell & Environment*, 37, 1338–1350.
- Zhang, F. (2003). A network of redundant bHLH proteins functions in all TTG1-dependent pathways of *Arabidopsis*. *Development*, 130, 4859–4869.
- Zhang, J. Y., He, S. B., Li, L., & Yang, H. Q. (2014). Auxin inhibits stomatal development through MONOPTEROS repression of a mobile peptide gene STOMAGEN in mesophyll. *Proceedings of the National Academy of Sciences of the United States of America*, 111, 3015–3023.
- Zhang, M., Zheng, X., Song, S., Zeng, Q., Hou, L., Li, D., ... Pei, Y. (2011). Spatiotemporal manipulation of auxin biosynthesis in cotton ovule epidermal cells enhances fiber yield and quality. *Nature Biotechnology*, 29, 453–458.
- Zhang, W., Wang, S., Yu, F., Tang, J., Shan, X., Bao, K., ... Li, J. (2019). Genome-wide characterization and expression profiling of SWEET genes in cabbage (*Brassica oleracea var. capitata* L.) reveal their roles in chilling and clubroot disease responses. *BMC Genomics*, 20, 93.
- Zhang, X. L., Yan, F., Tang, Y. W., Yuan, Y. J., Deng, W., & Li, Z. G. (2015). Auxin response gene SIARF3 plays multiple roles in tomato development and is involved in the formation of epidermal cells and trichomes. *Plant Cell and Physiology*, 56(11), 2110–2124.
- Zhao, Y., Huang, L. H., Peng, Y., Peng, Z. Z., Liu, X. Z., Kuang, F. C., ... Zhang, X. W. (2012). Trichome expression of *iaaM* transgene influences their development and elongation in tobacco. *Russian Journal of Plant Physiology*, 60, 839–844.
- Zhao, Y., Wang, J., Liu, Y., Miao, H., Cai, C., Shao, Z., ... Wang, Q. (2015). Classic myrosinase-dependent degradation of indole glucosinolate attenuates fumonisin B1-induced programmed cell death in *Arabidopsis*. *The Plant Journal*, 81, 920–933.

SUPPORTING INFORMATION

Additional supporting information may be found online in the Supporting Information section at the end of this article.

How to cite this article: Xuan L, Yan T, Lu L, et al. Genome-wide association study reveals new genes involved in leaf trichome formation in polyploid oilseed rape (*Brassica napus* L.). *Plant Cell Environ*. 2019;1–17. <https://doi.org/10.1111/pce.13694>